Bread & Butter Physics at the LHC

C.-P. Yuan
Michigan State University
Wu-Ki Tung Professorship in Particle Physics

July 18, 2025 @ Shandong University, China

In collaboration with CTEQ-TEA members

CTEQ – Tung et al. (TEA)
in memory of Prof. Wu-Ki Tung

The title of this talk was suggested by Prof. Tai Han for Pheno 2023 Symposium.

CTEQ-TEA group

CTEQ: The Coordinated Theoretical-Experimental Project on QCD

C T E Q

- CTEQ – Tung Et Al. (TEA)

in memory of Prof. Wu-Ki Tung, who co-established CTEQ Collaboration in early 90's

- Current members and collaborators:

China: Sayipjamal Dulat, Ibrahim Sitiwaldi, Alim Albet (Xinjiang U.), Tie-Jiun Hou (U. of South China), Liang Han, Minghui Liu, Siqi Yang (USTC) and other coauthors.

Mexico: Aurore Courtoy (Unam, Mexico)

USA: Marco Guzzi (Kennesaw State U.), Tim Hobbs (Argonne Lab), Pavel Nadolsky (Southern Methodist U.), Yao Fu, Joey Huston, Huey-Wen Lin, Max Ponce-Chavez, Dan Stump, Carl Schmidt, Keping Xie, C.-.P Yuan (Michigan State U.) and other coauthors.

Some useful websites:

- CT18 PDFs — https://ct.hepforge.org/PDFs/ct18/
- L2 Sensitivity — https://ct.hepforge.org/PDFs/ct18/figures/L2Sensitivity/
- ePump — https://epump.hepforge.org/
- ResBos2 — https://gitlab.com/resbos2

What is the bread-and-butter physics at the LHC?

The **bread and butter** of a situation or activity is its most ***basic*** or ***important*** aspects. --- Dictionary

- **Goals:** 1. Test Standard Model (SM)
  2. Find New Physics (NP)

Resonance search

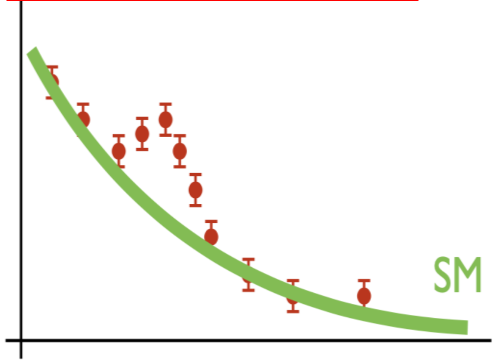

Deviation search

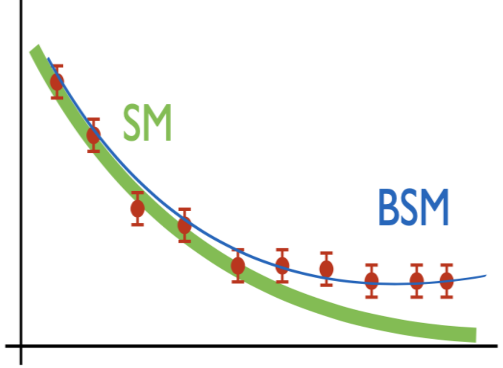

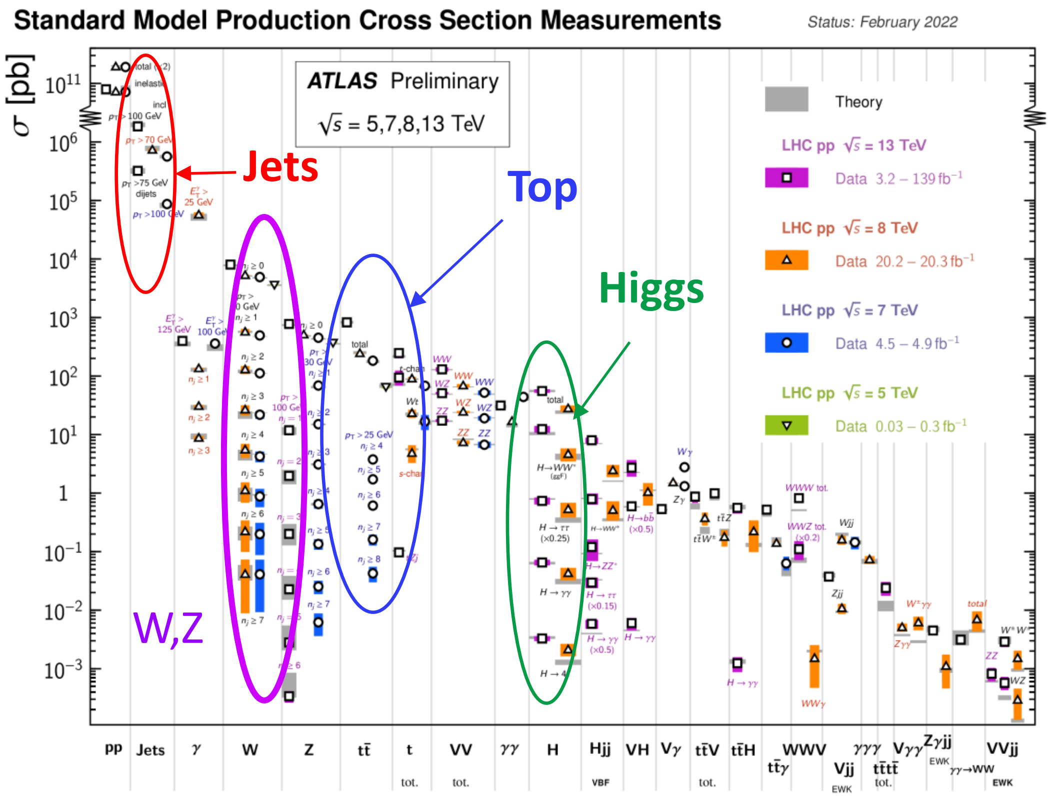

New Physics Found (in 1996) ?

C T E Q

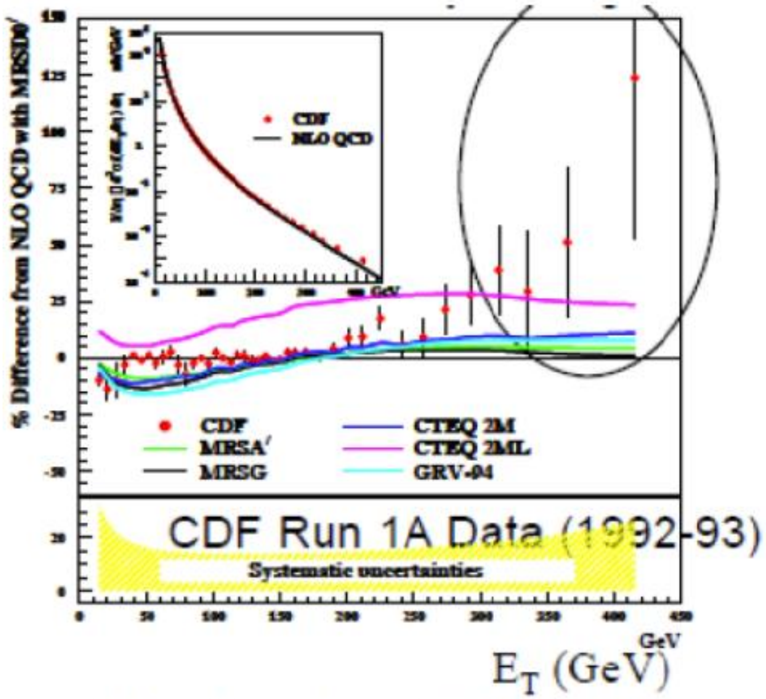

Phys. Rev. Lett. 77, 438 (1996)

High-x gluon not well known

...can be accommodated in the Standard Model

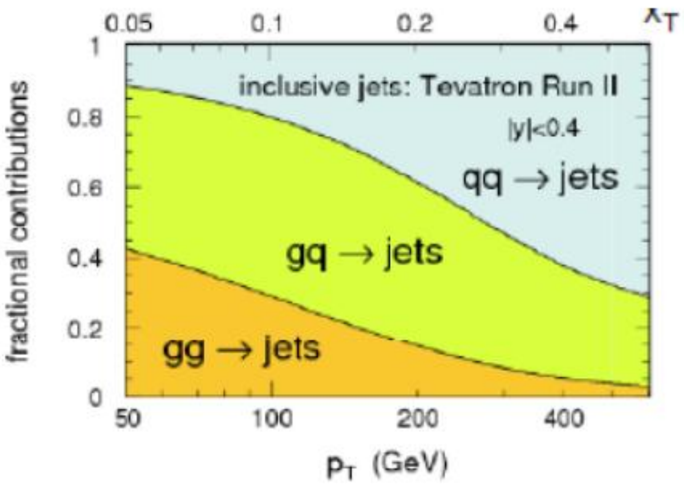

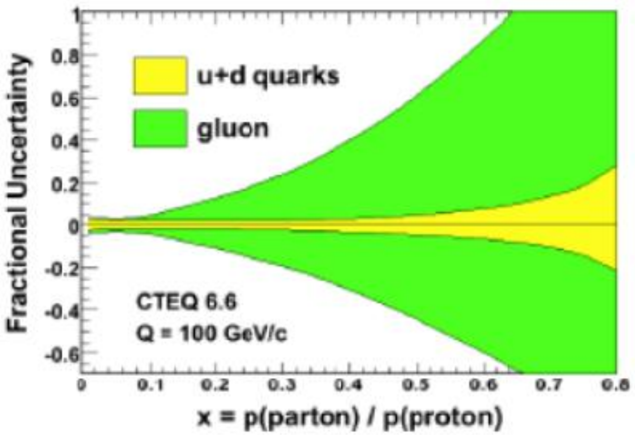

Explained by having better determined PDFs from global analysis;
no need for
NP scenario yet.

J. Huston, E. Kovacs, S. Kuhlmann, J.L. Lai, J.F. Owens, D. Soper, W.K. Tung , Phys. Rev. Lett. 77 (1996) 444.

Content

Part I:

QCD Factorization and

Parton Distribution Functions (PDFs)

Part II:

QCD Global analysis of PDFs

QCD Factorization and Parton Distribution Functions

Finding the Quarks at SLAC-MIT (1968)

- The quark structure of proton was first revealed by the SLAC-MIT deep inelastic scattering (DIS) experiments of high energy electrons on protons and bound neutrons.
- The exp data showed that the probability of deep inelastic scattering, where the electron lose a large fraction of its energy and emerges at a high scattering angle, was much greater than expected. The results were surprising to many as the proton appeared to be behaving as made up of point-like objects which respond independently to the high energy impinging electrons.
- The interpretation in terms of point-like scatterers followed from the scaling property predicted by Bjorken a couple of years earlier.

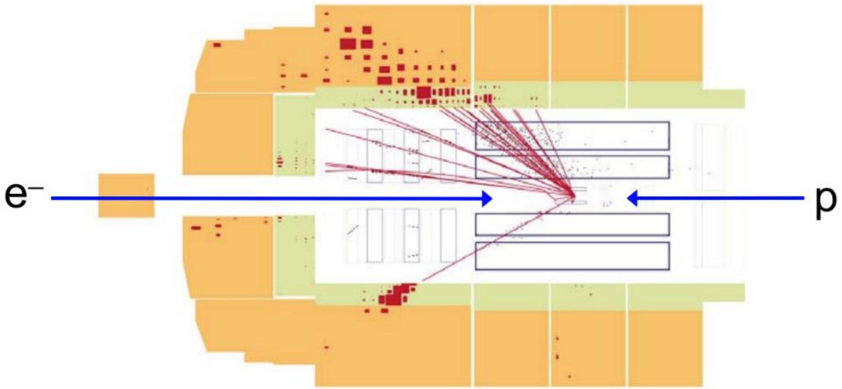

SLAC-MIT

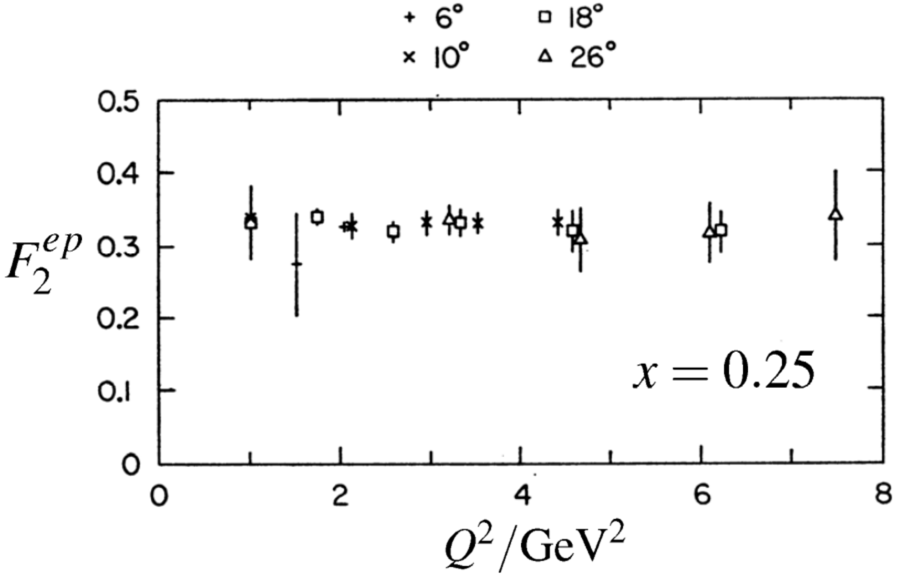

Feynman's Parton Model (1969)

- The Parton Model was proposed by Feynman to interpret the Bjorken scaling, observed in the SLAC-MIT experiment, as the point-like nature of the nucleon's constituents (i.e., partons) when they were incoherently scattered by the incident electron. Namely, in the large momentum transfers, the underlying process is elastic scattering off a point-like parton of mass, charge and spin.
- These point-like partons were later identified experimentally as (anti)quarks, which have fractional electric charge (2/3 or -1/3 for up and down quarks, respectively) with spin ½.

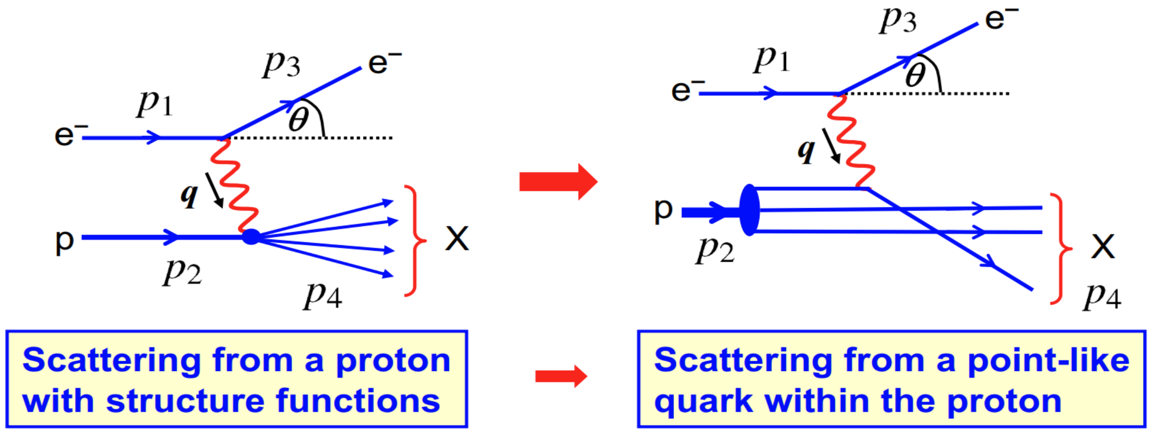

Protons consist of point-like spin-half constituents (quarks).

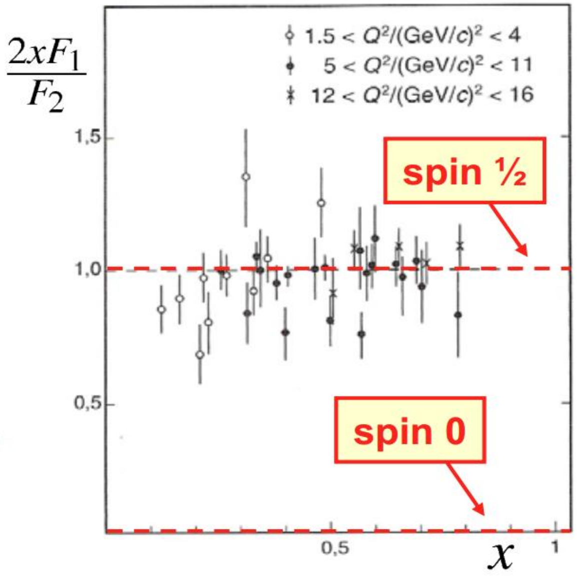

Callan-Gross relation

The Naive Parton Model

1969

Feynman

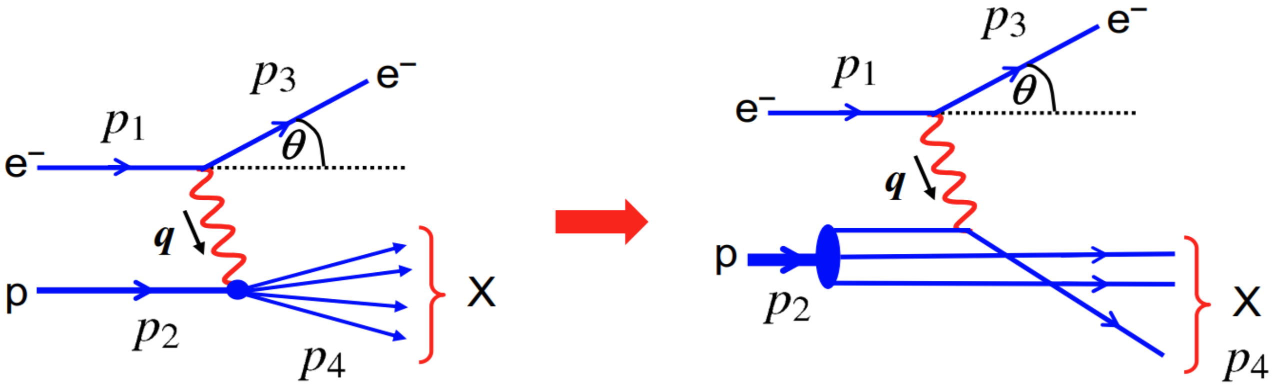

Scattering from a proton with structure functions → **Scattering from a point-like quark within the proton**

$$\int_0^1 x\left[u(x)+\overline{u}(x)+d(x)+\overline{d}(x)+s(x)+\overline{s}(x)\right]\mathrm{d}x \simeq 0.45.$$

- There must exist neutral quanta which contribute about 55% to the momentum of a fast-moving proton.
- The strong interactions could be described by a non-abelian gauge theory, in which the neutral quanta are the gluons.

Quantum Chromodynamics (QCD) is a Yang-Mills non-Abelian Gauge Theory

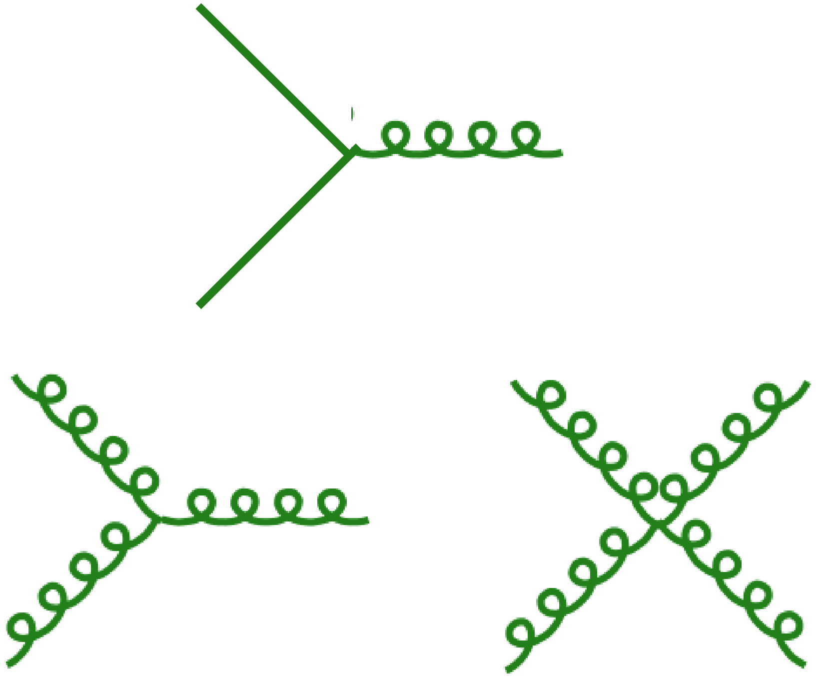

in which the carrier particles of a force can themselves radiate further carrier particles. (This is different from Quantum Electrodynamics, QED, where the photons that carry the electromagnetic force do not radiate further photons.)

$SU(3)_{colour}$

Gauge boson (gluon) Self-interactions

Quarks have 3 colors, gluon have 8 colors.
However, hadrons have to be colorless.

The First QCD Lagrangian

In 1971 Fritzsch and Gell-Mann introduced the color quantum number as the exact symmetry underlying the strong interactions. In 1972, Fritzsch and Gell-Mann proposed a Yang–Mills gauge theory with local color symmetry, which is now called quantum chromodynamics (QCD).

Harald Fritzsch (1943-2022) Murray Gell-Mann (1929-2019)

Harald Fritzsch, Murray Gell-Mann, *ICHEP 72* (1972), hep-ph/0208010
H. Fritzsch, Murray Gell-Mann, H. Leutwyler, *Phys.Lett.B* 47 (1973) 365

$$\mathcal{L} = \bar{q}\left[i\gamma^\mu\left(\partial_\mu + ig_s\frac{\lambda^A}{2}\mathcal{A}_\mu^A\right) - m\right]q - \frac{1}{4}F_{\mu\nu}^A F^{A\,\mu\nu}$$

$$F_{\mu\nu}^A = \partial_\mu\mathcal{A}_\nu^A - \partial_\nu\mathcal{A}_\mu^A - g_s f_{ABC}\mathcal{A}_\mu^B\mathcal{A}_\nu^C$$

λ^A are Gell-Mann matrices
f_{ABC} are called SU(3) structure constants

This publication, together with papers by Gross, Politzer and Wilczek about asymptotic freedom in non-Abelian gauge theories, is regarded as the beginning of QCD.

Perturbative QCD

- QCD was shown in 1973 to have a unique property of asymptotic freedom that its coupling constant decreases logarithmically with momentum scale.

Politzer, Gross, Wilczek, 2004 Nobel Prize

Asymptotic freedom of QCD

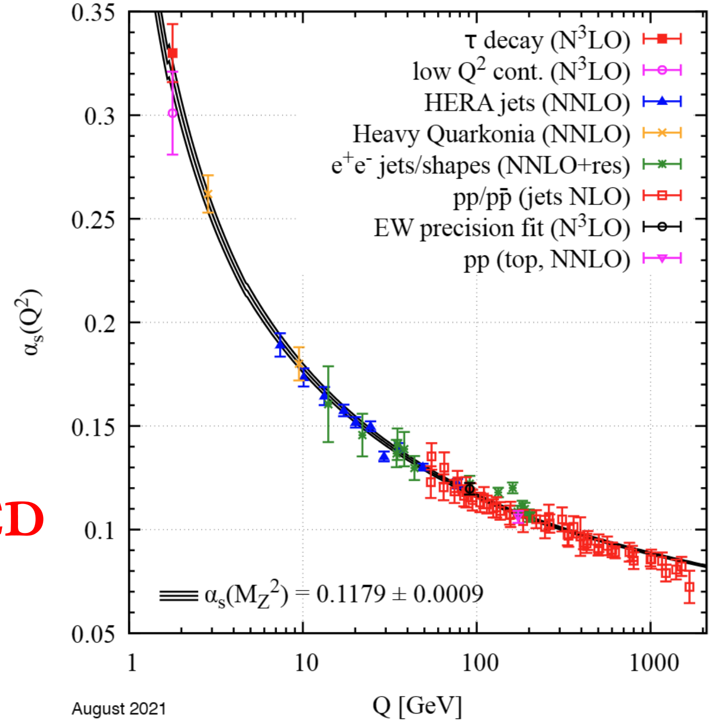

- 1979 DESY(the TASSO Collaboration at PETRA): confirm gluon in $e^+ e^-$ ->3 jets

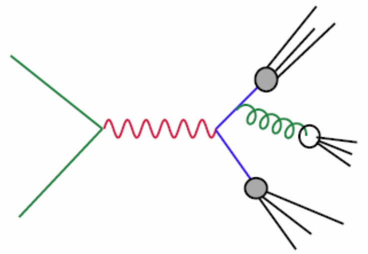

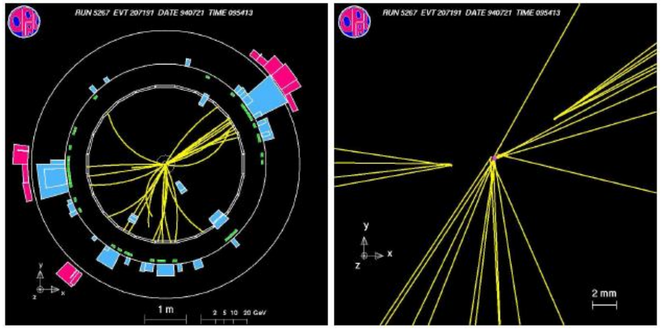

Nonperturbative QCD
Gluons bind quarks together inside proton

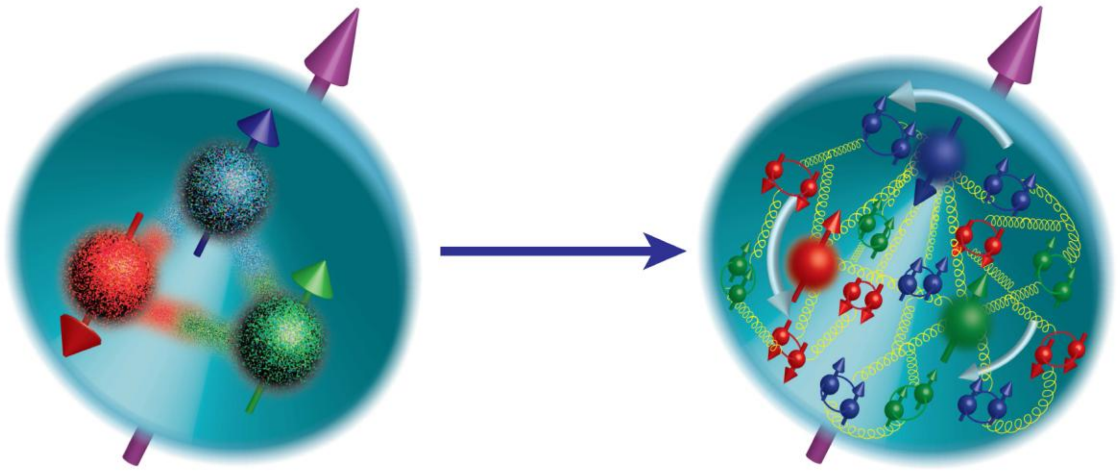

Constituent quarks

Current (anti-)quarks (valence and sea) and gluons

- The quarks are stuck together by the exchange of gluons.
- At low energy, one cannot see free quarks. The quarks are confined inside the proton due to color confinement. This is the nonperturbative nature of QCD interaction: QCD Confinement.

- At high energy, QCD has the unique property of asymptotically freedom.
- Asymptotic freedom ensures that when QCD is probed over short enough distances and times, it is well described by weakly interacting quarks and gluons. This is the perturbative nature of QCD interaction.

QCD Factorization and PDFs

$$\sigma_{pp\to H\to\gamma\gamma X}(Q) = \sum_{a,b=g,q,\bar{q}} \int_0^1 d\xi_a \int_0^1 d\xi_b \hat{\sigma}_{ab\to H\to\gamma\gamma}\left(\frac{x_a}{\xi_a}, \frac{x_b}{\xi_b}, \frac{Q}{\mu_R}, \frac{Q}{\mu_F}; \alpha_s(\mu_R)\right)$$
$$\times f_a(\xi_a, \mu_F) f_b(\xi_b, \mu_F) + O\left(\frac{\Lambda_{QCD}^2}{Q^2}\right)$$

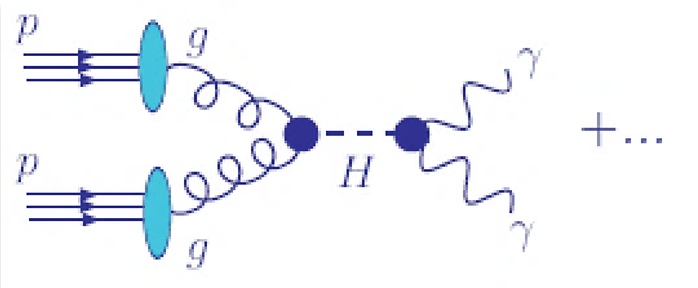

$\hat{\sigma}$ is the hard cross section; computed order-by-order in $\alpha_s(\mu_R)$
$f_a(x, \mu_F)$ is the distribution for parton a with momentum fraction x, at scale μ_F

$$f_{a/h}(x, Q)$$

Unpolarized collinear parton distribution functions (PDFs) $f_{a/h}(x, Q)$ are associated with probabilities for finding a parton a with the "+" momentum xp^+ in a hadron h with the "+" momentum p^+ for $p^+ \to \infty$, at a resolution scale $Q >$ 1 GeV .

The (unpolarized) collinear PDFs describe long-distance dynamics of (single parton scattering) in high-energy collisions.

Lepton-hadron Sc.

Master Equation for QCD Parton Model – the Factorization Theorem

$$F_A^\lambda\left(x, \frac{m}{Q}, \frac{M}{Q}\right) = \sum_a f_A^a\left(x, \frac{m}{\mu}\right) \otimes \hat{F}_a^\lambda\left(x, \frac{Q}{\mu}, \frac{M}{Q}\right) + \mathcal{O}\left(\left(\frac{\Lambda}{Q}\right)^2\right)$$

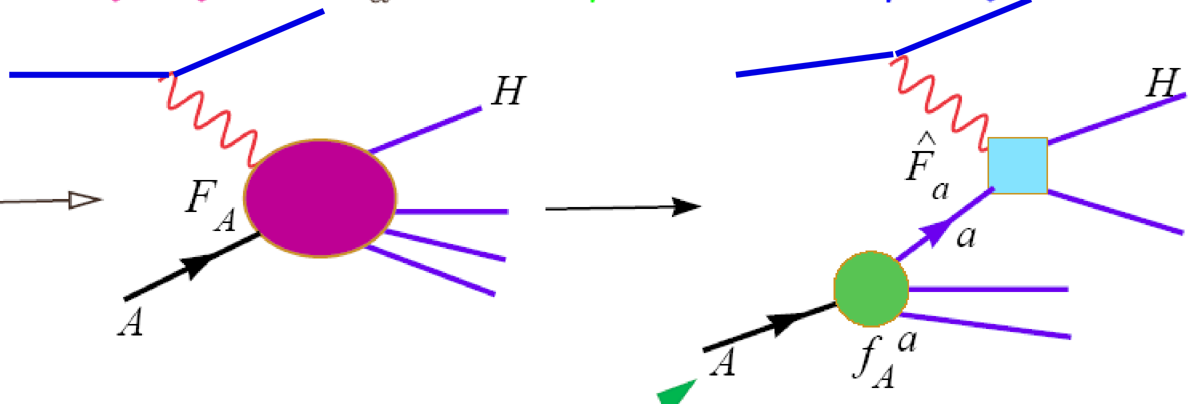

Experimental Input

Theory Input

Hard Cross-section
perturbative, calculable
(may contain $\alpha_s^n \mathrm{Log}^n(M/Q)$)

universal Parton Dist. Fn.
Non-Perturbative Parametrization at Q_0
DGLAP Evolution to Q

Extracted by global analysis

QCD Factorization and Parton Distribution Functions

Zhite Yu

Jefferson Lab

Winner of the 2024 J. J. and Noriko Sakurai Dissertation Award in Theoretical Particle Physics, the American Physics Society

Ph.D. Thesis (Spring 2023, MSU):
https://pa.msu.edu/graduate-program/current-graduate-students/thesis_ZhiteYu.pdf

To be inserted from another set of slides prepared by Zhite Yu

QCD Factorization and Parton Distribution Functions

Zhite Yu

Prepared for C.-P.'s lecture at
CTEQ Summer School
in 2022

Outline

Part I Factorization of DIS

Part II Definitions of parton distribution functions

Part III Renormalization of PDFs

Outline

Part I Factorization of DIS

Part II Definitions of parton distribution functions

Part III Renormalization of PDFs

DIS kinematics

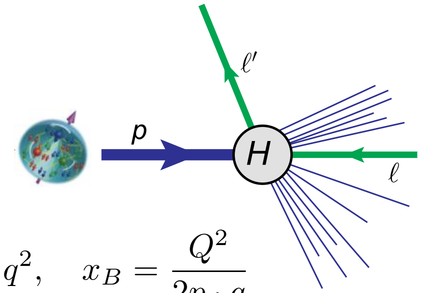

- **Kinematic observable is defined by the final-state lepton ℓ'**

3 independent variables. Many different choices.

- **Most standard:** $(Q^2,\ x_B,\ \phi_\ell)$ **or** $(x_B, y,\ \phi_\ell)$
- **Also possible:** $(y_\ell,\ p_T = \sqrt{\boldsymbol{\ell}_T'^2},\ \phi_\ell)$

$$q = \ell - \ell', \quad Q^2 = -q^2, \quad x_B = \frac{Q^2}{2p \cdot q}$$

$$y = \frac{p \cdot q}{p \cdot \ell} = \frac{Q^2}{x_B(s - m^2)}, \quad y_\ell = \frac{1}{2} \ln\left(\frac{\ell'^0 + \ell'^3}{\ell'^0 - \ell'^3}\right)$$

Lepton phase space:

$$d\sigma = \frac{1}{2\,(s - m^2)} \frac{d^3\boldsymbol{\ell}'}{(2\pi)^3 2E'} \overline{|\mathcal{M}|^2} = \frac{y^2}{Q^2} \frac{dx_B\, dQ^2\, d\phi_\ell}{(4\pi)^3} \overline{|\mathcal{M}|^2} = \frac{y\, dx_B\, dy\, d\phi_\ell}{(4\pi)^3} \overline{|\mathcal{M}|^2} = \frac{dy_\ell\, dp_T^2\, d\phi_\ell}{(4\pi)^3 (s - m^2)} \overline{|\mathcal{M}|^2}$$

Advantage for using $(Q^2,\ x_B,\ \phi_\ell)$

- **Lorentz invariant**
- **Makes "deep inelastic" region manifest:** $Q^2 > Q_0^2, \quad W = (p+q)^2 = m^2 + Q^2\left(\frac{1}{x_B} - 1\right) > W_0$
- **Takes advantage of one-photon exchange approximation (LO QED)**

Basic intuition: Feynman's Parton Model

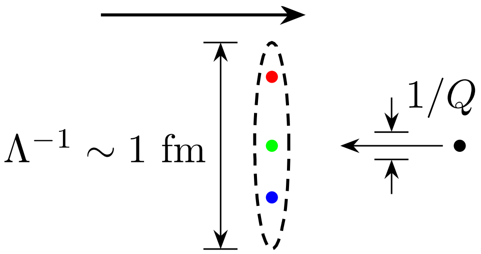

- Interaction happens locally:
$$\tau \sim 1/Q$$
- Hadron has size:
$$1/\Lambda \sim \text{fm}$$
- Time dilation:
$$Q/\Lambda$$

The interaction among the partons happens in a time scale $\frac{Q}{\Lambda}\frac{1}{\Lambda} \gg \tau$

1. Electron only hits one "parton" in the hadron;
2. Parton is a free on-shell particle;

$$\sigma = \sum_i \int dx\, f_i(x)\hat{\sigma}_i(x)$$

For a second parton to enter the interaction, there is a penalty $\frac{1/Q}{1/\Lambda} = \frac{\Lambda}{Q}$

Indication: "Parton model" is correct up to *power corrections.*

LO illustration of DIS factorization

Frame choice:
Breit frame

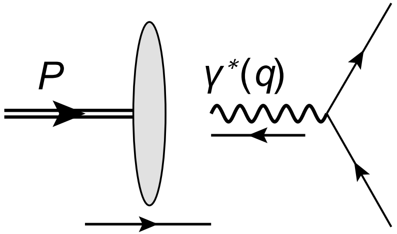

Convenient for factorization:

- Simple power counting:
  $P^+ \gg P^-, P_T$
- Clearer physical picture:
  Lorentz contracted along z

Note: Factorization formula does not depend on frame, but a good frame choice can simplify our analysis.

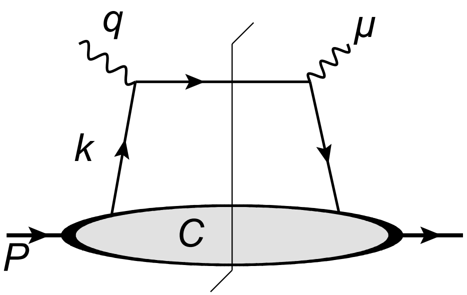

Pinch singular surface (PSS) for the massless theory

$$P = \left(P^+, 0, \mathbf{0}_T\right),$$
$$q = \left(-x\,P^+, \frac{Q^2}{2\,x\,P^+}, \mathbf{0}_T\right),$$
$$k = \left(\xi\,P^+, 0, \mathbf{0}_T\right).$$

Light-cone coordinates

MICHIGAN STATE UNIVERSITY

For a general 4-vector V^μ, we define

$$V^+ = n \cdot V = \frac{V^0 + V^3}{\sqrt{2}}, \; V^- = \bar{n} \cdot V = \frac{V^0 - V^3}{\sqrt{2}}, \; \boldsymbol{V}_T = (V^1, V^2)$$

$$V = (V^+, V^-, \boldsymbol{V}_T)$$

$$n = (0^+, 1^-, \boldsymbol{0}_T), \; \bar{n} = (1^+, 0^-, \boldsymbol{0}_T).$$

$$n^\mu = \frac{1}{\sqrt{2}}(1, 0, 0, -1), \; \bar{n}^\mu = \frac{1}{\sqrt{2}}(1, 0, 0, 1)$$

$$V \cdot W = V^+ W^- + V^- W^+ - \boldsymbol{V}_T \cdot \boldsymbol{W}_T,$$

$$V^2 = 2V^+ V^- - \boldsymbol{V}_T^2.$$

Factorization: Pick up the dominant contribution

It is near the PSS that we get dominant contribution.

PSS: $k = (\xi P^+, 0, 0_T)$ neighborhood

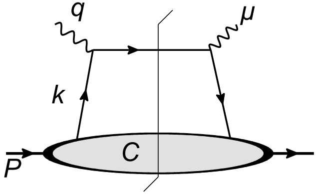

$$k = (k^+, k^-, \boldsymbol{k}_T)$$
$$k^+ \sim \mathcal{O}(Q),\ k^-, k_T \ll Q$$

Leading region

Task: pick up the dominant contribution in this region

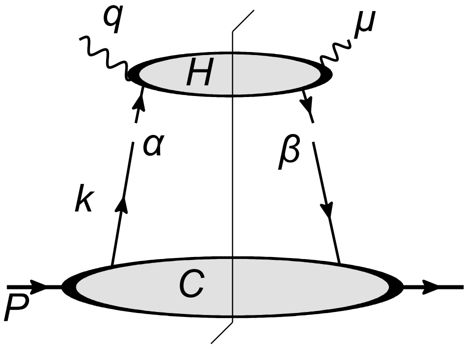

$$W^{\mu\nu}(x, Q^2) = \int \frac{d^4k}{(2\pi)^4} H^{\mu\nu}_{\beta\alpha}(q,k)\, C_{\alpha\beta}(k,P)$$

$$C_{\alpha\beta}(k,P) = \int d^4x\, e^{-ik\cdot w} \langle P|\, \overline{\psi}_\beta(w)\, \psi_\alpha(0)\, |P\rangle$$

Approximation One:

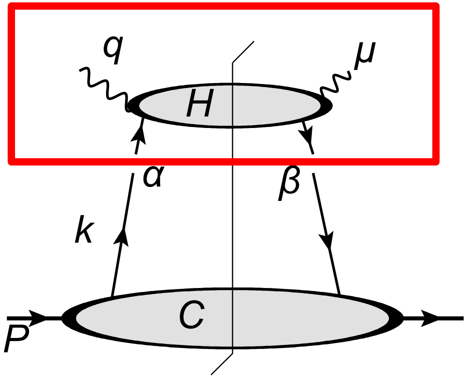

Neglect the small components of k in H

- In H: $k \to \hat{k} = (k^+, 0, \mathbf{0}_T)$
- $H(k,q) \to H(\hat{k},q)$

$$W^{\mu\nu}(x,Q^2) = \int \frac{d^4k}{(2\pi)^4} H^{\mu\nu}_{\beta\alpha}(q,k)\, C_{\alpha\beta}(k,P)$$
$$\simeq \int dk^+\, H^{\mu\nu}_{\beta\alpha}(q,\hat{k}) \left[\int \frac{dk^- d^2\boldsymbol{k}_T}{(2\pi)^4} C_{\alpha\beta}(k,P) \right]$$

Momentum k^-, k_T are disentangled

Spinor indices are still entangled

Approximation Two:

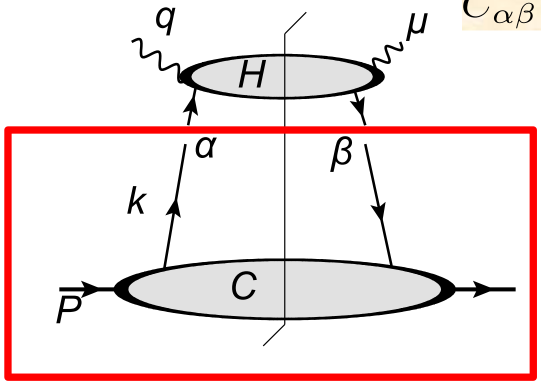

$$C_{\alpha\beta}(k,P) = S\,\mathbf{1}_{\alpha\beta} + A\,(\gamma_5)_{\alpha\beta} + V^{\mu}\,(\gamma_\mu)_{\alpha\beta} + A^{\mu}\,(\gamma_5\gamma_\mu)_{\alpha\beta} + T^{\mu\nu}\,(\sigma_{\mu\nu})_{\alpha\beta}$$

- In Breit frame, $k^+, P^+ \sim Q$.
- In rest frame, k^μ, $P^\mu \sim m$. $S \sim A \sim V^\mu \sim A^\mu \sim T^{\mu\nu}$
- Boost from rest frame to Breit frame
  - $S,\ A$: not changed;
  - $V^+,\ A^+,\ T^{+i}$: enhanced by Q/m;
  - $V^-,\ A^-,\ T^{-i}$: suppressed by m/Q;
  - $V_T,\ A_T,\ T^{+-},\ T^{ij}$: not changed

Only keep $V^+,\ A^+,\ T^{+i}$

$$C \simeq V^+\gamma_+ + A^+\gamma_5\gamma_+ + T^{+i}\sigma_{+i}$$

$$V^+ = \frac{1}{4}\,\mathrm{Tr}\left[\gamma^+ C\right]$$

$$A^+ = \frac{1}{4}\,\mathrm{Tr}\left[\gamma^+\gamma_5\, C\right]$$

$$T^{+i} = \frac{1}{8}\,\mathrm{Tr}\left[\sigma^{+i}\, C\right]$$

Factorized result

$$W^{\mu\nu}(x,Q^2) \simeq \int \frac{dk^+}{k^+}\left[\mathrm{Tr}\left(H^{\mu\nu}(q,\hat{k})\frac{k^+\gamma^-}{2}\right) f(\xi) + \mathrm{Tr}\left(H\,\frac{k^+\gamma_5\gamma^-}{2}\right)\Delta f(\xi) + \mathrm{Tr}\left(H\,\frac{k^+\sigma^{i-}}{2}\right)\delta_T^i f(\xi)\right]$$
$$= \int_x^1 \frac{d\xi}{\xi}\left[\mathrm{Tr}\left(H^{\mu\nu}(q,\hat{k})\frac{\hat{\not k}}{2}\right) f(\xi) + \mathrm{Tr}\left(H\,\frac{\gamma_5\hat{\not k}}{2}\right)\Delta f(\xi) + \mathrm{Tr}\left(H\,\frac{\sigma^{i\hat{k}}}{4}\right)\delta_T^i f(\xi)\right]$$

unpolarized $\quad f(\xi) = \int \frac{dk^- d^2\boldsymbol{k}_T}{(2\pi)^4}\,\mathrm{Tr}\left[\frac{\gamma^+}{2}C(k,P)\right] = \int \frac{dw^-}{2\pi} e^{-i\xi P^+ w^-}\left\langle P\left|\overline{\psi}(0^+,w^-,\mathbf{0}_T)\frac{\gamma^+}{2}\psi(0)\right|P\right\rangle$

helicity $\quad \Delta f(\xi) = \int \frac{dk^- d^2\boldsymbol{k}_T}{(2\pi)^4}\,\mathrm{Tr}\left[\frac{\gamma^+\gamma_5}{2}C(k,P)\right] = \int \frac{dw^-}{2\pi} e^{-i\xi P^+ w^-}\left\langle P,S\left|\overline{\psi}(0^+,w^-,\mathbf{0}_T)\frac{\gamma^+\gamma_5}{2}\psi(0)\right|P,S\right\rangle$

transversity $\quad \delta_T^i f(\xi) = \int \frac{dk^- d^2\boldsymbol{k}_T}{(2\pi)^4}\,\mathrm{Tr}\left[\frac{\sigma^{+i}}{2}C(k,P)\right] = \int \frac{dw^-}{2\pi} e^{-i\xi P^+ w^-}\left\langle P,S\left|\overline{\psi}(0^+,w^-,\mathbf{0}_T)\frac{\sigma^{+i}}{2}\psi(0)\right|P,S\right\rangle$

spin vector

When $S = 0$, $\Delta f = \delta_T^i f = 0$.

$$W^{\mu\nu}(x,Q^2) = \int_x^1 \frac{d\xi}{\xi}\, f(\xi)\, C^{\mu\nu}(x/\xi, Q^2) + \mathcal{O}(m/Q)$$

Complete?

In full QCD, this is far from complete.

- QCD is a renormalizable theory, $[g] = 0$.
  - $\Longrightarrow$ High-order corrections are also leading
  - $\Longrightarrow$ Factorization scale
- QCD is a gauge theory: massless vector boson.
  - $\Longrightarrow$ More gluons can attach C to H
  - $\Longrightarrow$ Wilson line: gauge-invariant PDFs

all possible diagrams

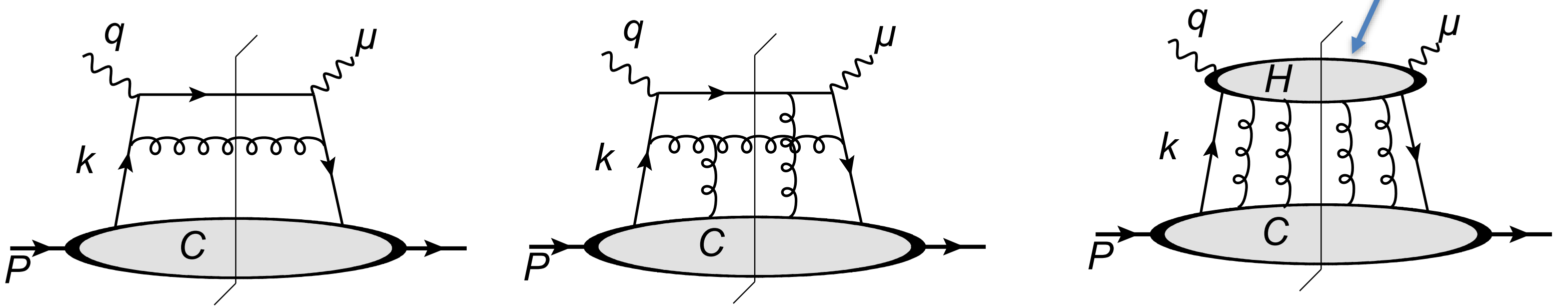

Outline of all-order DIS factorization

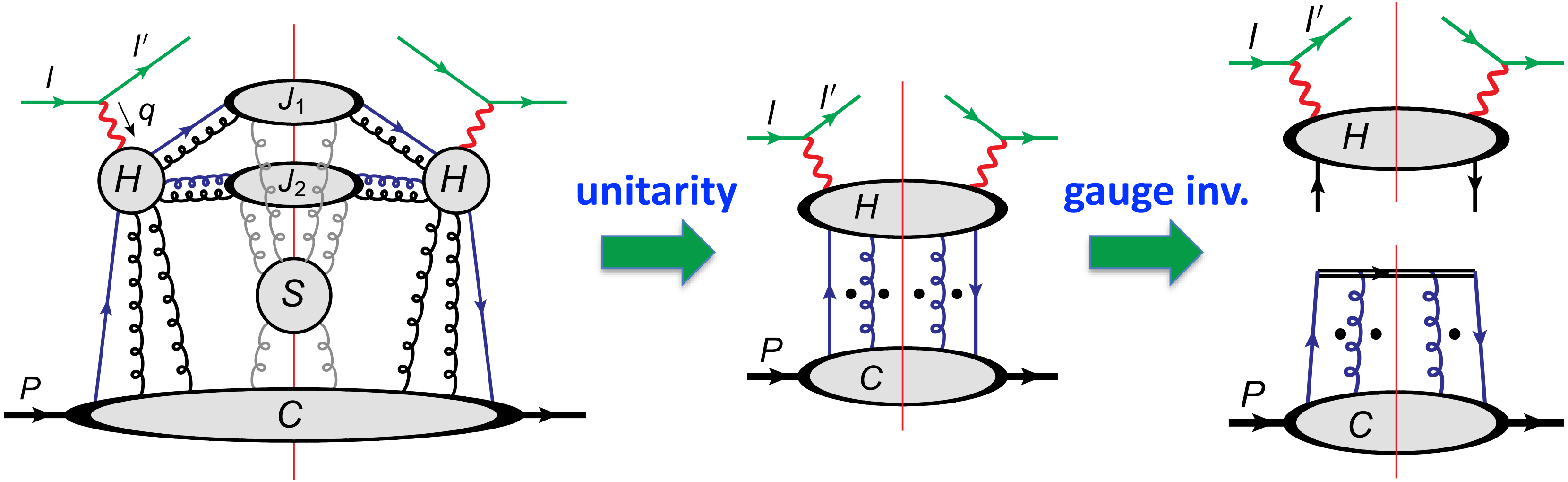

Parton distribution function (PDF)

$$f_q(x) = \int_{-\infty}^{\infty} \frac{dy^-}{4\pi} e^{-ixP^+y^-} \langle P|\bar{\psi}(y^-)\gamma^+ W_n(y^-,0)\psi(0)|P\rangle \qquad V^\pm = \frac{V^0 \pm V^3}{\sqrt{2}}$$

$f_q(x)dx =$ **# partons q with longitudinal momentum fraction in $(x, x+dx)$**

Outline

Part I Factorization of DIS

Part II Definitions of parton distribution functions

Part III Renormalization of PDFs

Recap: DIS factorization

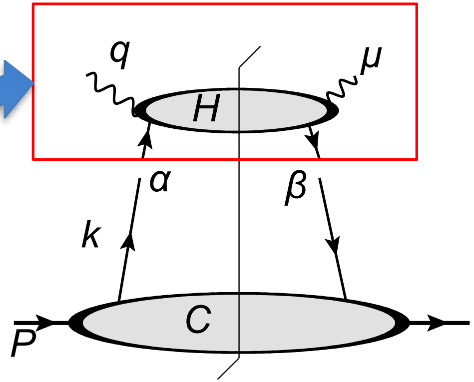

$$W^{\mu\nu}(x,Q^2) = \int \frac{d^4k}{(2\pi)^4} H^{\mu\nu}_{\beta\alpha}(q,k)\, C_{\alpha\beta}(k,P)$$

$$C_{\alpha\beta}(k,P) = \int d^4w\, e^{-ik\cdot w} \langle P|\, \overline{\psi}_\beta(w)\, \psi_\alpha(0)\, |P\rangle$$

- In H: $k \to \hat{k} = (k^+, 0, \mathbf{0}_T)$
- $H(k,q) \to H(\hat{k},q)$

$$W^{\mu\nu}(x,Q^2) \simeq \int dk^+\, H^{\mu\nu}_{\beta\alpha}(q,\hat{k}) \left[\int \frac{dk^- d^2\boldsymbol{k}_T}{(2\pi)^4} C_{\alpha\beta}(k,P)\right]$$

Recap: DIS factorization

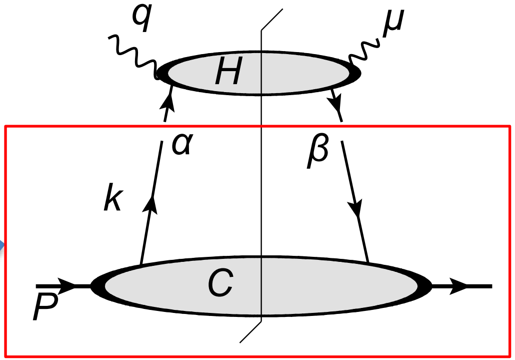

$$W^{\mu\nu}(x,Q^2) = \int \frac{d^4k}{(2\pi)^4} H^{\mu\nu}_{\beta\alpha}(q,k)\, C_{\alpha\beta}(k,P)$$

$$C_{\alpha\beta}(k,P) = \int d^4w\, e^{-ik\cdot w}\, \langle P|\, \overline{\psi}_\beta(w)\, \psi_\alpha(0)\, |P\rangle$$

$$W^{\mu\nu}(x,Q^2) \simeq \int dk^+\, H^{\mu\nu}_{\beta\alpha}(q,\hat{k}) \left[\int \frac{dk^- d^2\boldsymbol{k}_T}{(2\pi)^4} C_{\alpha\beta}(k,P)\right]$$

How?

$$\left[\int \frac{dk^- d^2\boldsymbol{k}_T}{(2\pi)^4} C_{\alpha\beta}(k,P)\right] = f(\xi)\frac{\gamma^-}{2} + \Delta f(\xi)\frac{\gamma_5\gamma^-}{2} + \delta_T^i f(\xi)\frac{\gamma^-\gamma^i\gamma_5}{2}$$

$$k^+ = \xi P^+$$

$$W^{\mu\nu}(x,Q^2) \simeq \int \frac{d\xi}{\xi} f(\xi)\cdot \mathrm{Tr}\left[H^{\mu\nu}(q,\hat{k})\frac{\hat{\not{k}}}{2}\right] + \text{polarized terms}$$

Parton density in terms of Green function

- Part of an amplitude

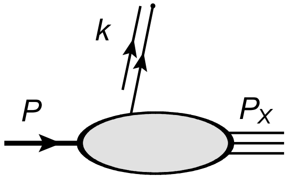

$$= M_L = \langle P_X, \mathrm{out}|\psi_\alpha(0)|P, \mathrm{in}\rangle$$

"amplitude" to get a parton with $k = P - P_X$

- Corresponding part of the complex conjugate diagram

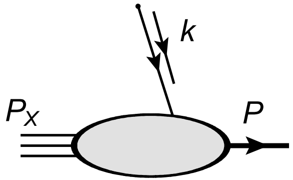

$$= M_R = \langle P, \mathrm{in}|\,\overline{\psi}_\beta(0)\,|P_X, \mathrm{out}\rangle = M_L^\dagger \gamma^0$$

- PDF = $M_R\, M_L$ with proper vertex

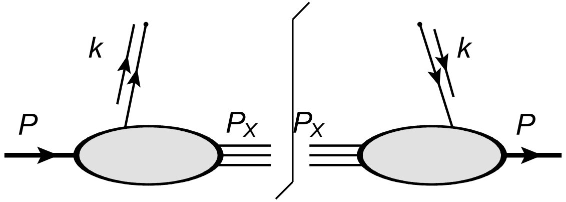

$$= \sum_X (2\pi)^4 \delta^{(4)}(P - k - P_X) M_R M_L$$

$$= \int d^4 w\, e^{-ik\cdot w} \langle P, \mathrm{in}|\,\overline{\psi}_\beta(w)\psi_\alpha(0)|P, \mathrm{in}\rangle = C_{\alpha\beta}(k, P)$$

PDF = cut diagram

Lesson: We can write the cut diagram as Green function in the same way as we do for an *uncut* diagram, but with *regular-ordered* operators

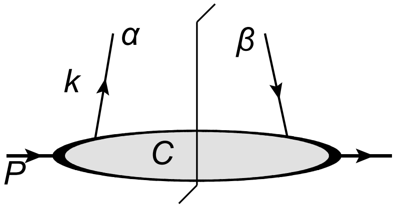

$$= C_{\alpha\beta}(k,P) = \int d^4w\, e^{-ik\cdot w}\, \langle P|\, \underbrace{\overline{\psi}_\beta(w)\, \psi_\alpha(0)}_{\textit{regular-ordered}}\, |P\rangle$$

$$\text{parton density} = \int \frac{dk^- d^2\boldsymbol{k}_T}{(2\pi)^4} C_{\alpha\beta}\Gamma_{\beta\alpha}$$

$$= \int \frac{dw^-}{2\pi} e^{-ik^+w^-} \langle P|\, \overline{\psi}_\beta(w^-)\Gamma_{\beta\alpha}\psi_\alpha(0)\, |P\rangle$$

- $\int dk^- d^2\boldsymbol{k}_T \Rightarrow \bar{\psi}$ and ψ are separated along light-cone.
- Different projection Γ leads to different parton densities.
- Only $\int dk^- \Rightarrow$ Transverse Momentum Dependent (TMD) parton density.

Statements of the results

- $\Gamma = \frac{\gamma^+}{2}$ gives unpolarized parton density

$$f_j(x) = \int \frac{dw^-}{2\pi} e^{-ixP^+w^-} \langle P| \overline{\psi}_j(w^-) \frac{\gamma^+}{2} \psi_j(0) |P\rangle$$

  - Physical meaning: $f_j(x)dx$ = # of partons j with k^+/P^+ in $x \sim x + dx$.
  - Check normalization

$$\int_{-\infty}^{\infty} dx f_j(x) = \frac{1}{2P^+} \langle P| \overline{\psi}_j(0)\gamma^+ \psi_j(0) |P\rangle = N_j - N_{\bar{j}}$$

- $\Gamma = \frac{\gamma^+\gamma_5}{2}$ gives helicity parton density

$$\Delta f_j(x) = \int \frac{dw^-}{2\pi} e^{-ixP^+w^-} \langle P| \overline{\psi}_j(w^-) \frac{\gamma^+\gamma_5}{2} \psi_j(0) |P\rangle$$

- $\Gamma = \frac{\gamma^+\gamma^i\gamma_5}{2}$ gives parton transversity

$$\delta_T^i f_j(x) = \int \frac{dw^-}{2\pi} e^{-ixP^+w^-} \langle P| \overline{\psi}_j(w^-) \frac{\gamma^+\gamma_T^i\gamma_5}{2} \psi_j(0) |P\rangle$$

Summarize: quark proton spin

$f(x) \;=$

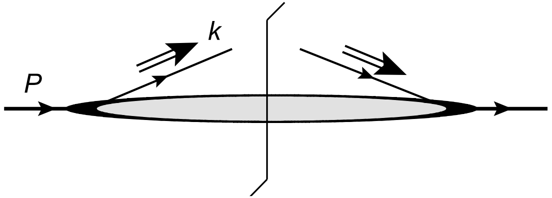

$+$

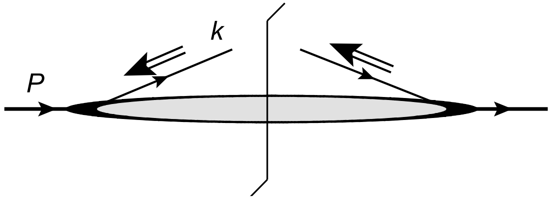

$\Delta f(x) \;=$

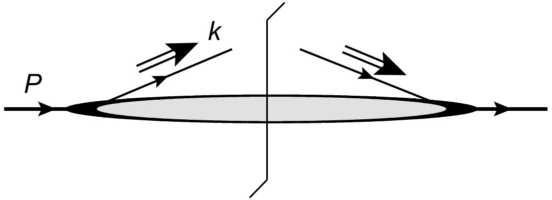

$-$

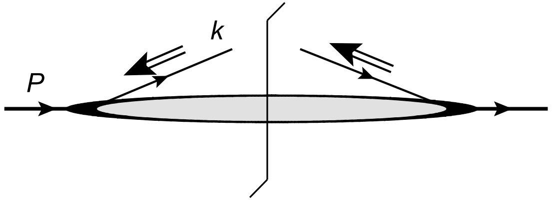

$\delta_T^x f(x) \;=$

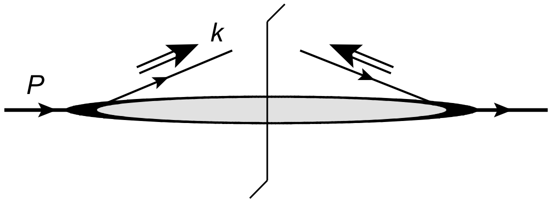

$+$

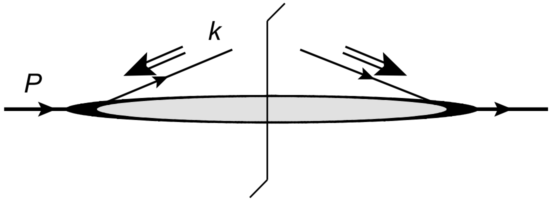

$\delta_T^y f(x) \;=\; i$

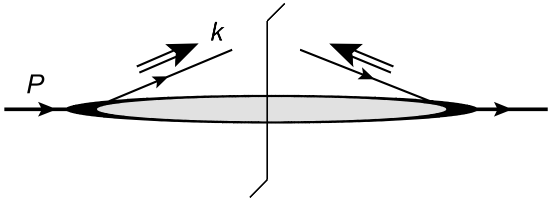

$-i$

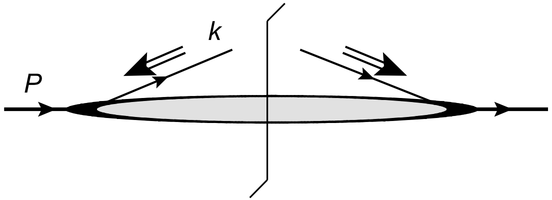

Unpolarized Quark PDF

$$f_q(x) = \int \frac{\mathrm{d}k^- \mathrm{d}^2\boldsymbol{k}_T}{(2\pi)^4}$$

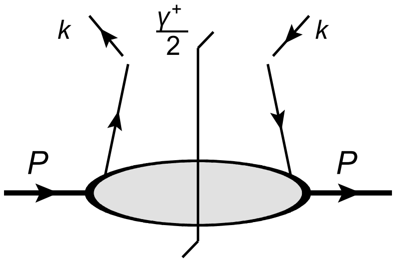

$$= \int_{-\infty}^{\infty} \frac{\mathrm{d}w^-}{2\pi} e^{-ixP^+w^-} \left\langle P \left| \overline{\psi}(0^+, w^-, \mathbf{0}_T) \frac{\gamma^+}{2} \psi(0) \right| P \right\rangle$$

$$\boxed{f_{i/P}(x) = \int_{-\infty}^{\infty} \frac{dw^-}{2\pi} e^{-ixP^+w^-} \left\langle P \left| \overline{\psi}_i(0^+, w^-, \mathbf{0}_T) \frac{\gamma^+}{2} W_F[w^-, 0]\, \psi_i(0) \right| P \right\rangle}$$

Wilson line:

$$\left(W_F[w^-, 0]\right)_{jk} = P \exp\left\{ -ig \int_0^{w^-} dy^- A_a^+(0^+, y^-, \mathbf{0}_T)(T_F^a)_{jk} \right\}$$

Unpolarized Gluon PDF

$$f_g(x) = \int \frac{\mathrm{d}k^- \mathrm{d}^2 \boldsymbol{k}_T}{(2\pi)^4}$$

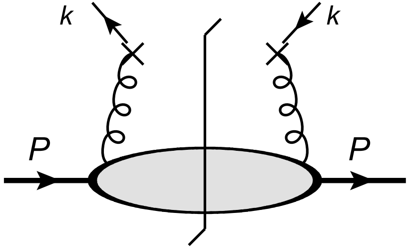

$$= \sum_{a} \sum_{j=1,2} \int_{-\infty}^{\infty} \frac{\mathrm{d}w^-}{2\pi x P^+} e^{-ixP^+w^-} \langle P|F^{a,+j}(w^-)F^{a,+j}(0)|P\rangle$$

To make it gauge invariant, Wilson line must be inserted:

$$(W_A[w^-, 0])_{bc} = P\exp\left\{-ig\int_0^{w^-} dy^- A_a^+(0^+, y^-, \mathbf{0}_T)(T_A^a)_{bc}\right\}$$

Outline

Part I Factorization of DIS

Part II Definitions of parton distribution functions

Part III Renormalization of PDFs

Recitation question

Where does the factorization scale μ_f come about in the definition of renormalized PDF, in collinear factorization?

Renormalization of PDFs

❑ Factorization and UV divergence

$$\int \frac{\mathrm{d}^4 k}{(2\pi)^4}$$

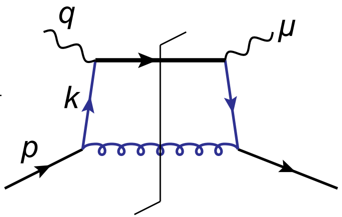

has no UV divergence: large k_T region is suppressed

factorization

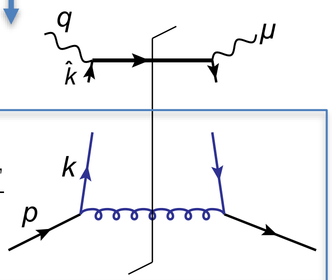

$$\boxed{\int \frac{\mathrm{d}k^- \mathrm{d}^2 \boldsymbol{k}_T}{(2\pi)^4}}$$

contains UV divergence as $k_T \to \infty$: logarithmic divergence

- Factorization: factorize collinear divergence into PDF
- But PDF contains extra (superficial) UV divergence that is not in the original cross section
- Need extra UV renormalization for the PDF

Renormalization of PDFs

❑ Method one: cutoff k_T integral

Factorization scale

$$\int \frac{\mathrm{d}k^- \mathrm{d}^2 \boldsymbol{k}_T}{(2\pi)^4} \to \int \frac{\mathrm{d}k^- \mathrm{d}^2 \boldsymbol{k}_T}{(2\pi)^4} \theta(\mu_f - k_T)$$

- **Clear physical picture: PDF only includes scale at $k_T \leq \mu_f$**
- **But not unambiguously extendable to higher orders in terms of actual calculation**

❑ Method two: Dim. Reg. + $\overline{\mathrm{MS}}$

$$\mu^{4-d} \int \frac{\mathrm{d}k^- \mathrm{d}^{d-2} \boldsymbol{k}_T}{(2\pi)^d}$$

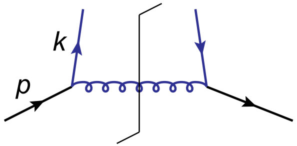

$$-\text{UV divergence } \left(\frac{1}{4-d} \text{ poles}\right) \quad = \text{renormalized PDF}$$

- **Effectively subtract contribution from the scale $k_T \gg \mu_f$, so that PDF only includes contribution from the scale $k_T \leq \mu_f$**
- **μ_f = factorization scale: scale above μ_f is included in the hard coefficient function**
- **Easily calculated and extended to higher orders**
- **Renormalized PDF (and hard coefficient) depends on the factorization scale μ_f**

Renormalization of PDFs

❑ Multiplicative renormalization

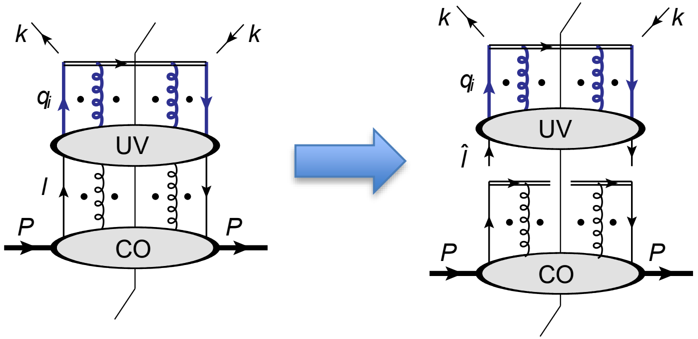

Renormalized PDF

Bare PDF

$$f_i(x,\mu) = \sum_{j=q,\bar{q},g} \int_x^1 \frac{\mathrm{d}z}{z} Z_{ij}(x/z, 1/\epsilon; \mu)\, f_j^0(z, 1/\epsilon)$$

Renormalization factor

❑ Renormalization group evolution (RGE)

Multiplicative renormalization

$$\frac{\mathrm{d}}{\mathrm{d}\ln\mu^2} Z_{ik}(z, 1/\epsilon, \alpha_s(\mu)) = \sum_{j=q,\bar{q},g} \int_z^1 \frac{\mathrm{d}y}{y} P_{ij}(z/y, \alpha_s(\mu))\, Z_{jk}(y, 1/\epsilon, \alpha_s(\mu))$$

Evolution equation of PDFs (DGLAP equations)

Evolution kernel

$$\frac{\mathrm{d}f_i(x,\mu)}{\mathrm{d}\ln\mu^2} = \sum_{j=q,\bar{q},g} \int_x^1 \frac{\mathrm{d}z}{z} P_{ij}(x/z, \alpha_s(\mu))\, f_j(z,\mu)$$

Calculation of DGLAP evolution kernel: 1-loop example

Example diagram

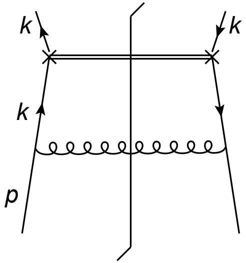

$$f_{q/q}^{(0)[1]}(x) = \int \frac{\mathrm{d}^d k}{(2\pi)^d}\, \delta(k^+ - xp^+)\, (-g^{\mu\nu})\, (2\pi)\delta\left((p-k)^2\right)\, \theta(p^+ - k^+) \times$$
$$\times \operatorname{Tr}\left[\frac{\gamma^+}{2} \frac{i\not{k}}{k^2 + i\varepsilon} \left(-ig\mu^\varepsilon \gamma_\mu t^a_{ji}\right) \frac{\not{p}}{2} \left(ig\mu^\varepsilon \gamma_\nu t^a_{ij}\right) \frac{-i\not{k}}{k^2 - i\varepsilon}\right]$$
$$= -g^2 \mu^{2\varepsilon} C_F \int \frac{\mathrm{d}k^- \mathrm{d}^{2-2\varepsilon}\boldsymbol{k}_T}{(2\pi)^d} (2\pi)\delta\left((p-k)^2\right) \frac{\operatorname{Tr}\left[\frac{\gamma^+}{2}\not{k}\gamma^\mu \frac{\not{p}}{2}\gamma_\mu \not{k}\right]}{(k^2 + i\varepsilon)(k^2 - i\varepsilon)}$$

Use δ-function to integrate out k^-: $\delta\left((k-p)^2\right) = \frac{1}{2(1-x)p^+}\delta\left(k^- + \frac{k_T^2}{2(1-x)p^+}\right)$

$$k = \left(xp^+,\ -\frac{k_T^2}{2(1-x)p^+},\ \boldsymbol{k}_T\right)$$

$$f_{q/q}^{(0)[1]}(x) = \frac{\alpha_s C_F}{2\pi} \frac{(4\pi\mu^2)^\varepsilon}{\Gamma(1-\varepsilon)} (1-\varepsilon)(1-x) \int \frac{\mathrm{d}k_T^2}{k_T^2} (k_T^2)^{-2\varepsilon}$$

Scaleless integral: $=$ UV $+$ IR $= 0$

$$\text{UV of } f_{q/q}^{(0)[1]}(x) = \frac{\alpha_s}{2\pi} C_F \frac{1}{\varepsilon}(1-x) = -Z_{qq}^{[1]}(x)$$

$$f_{q/q}^{[1]}(x) = f_{q/q}^{(0)[1]}(x) + Z_{qq}^{[1]}(x) = \text{IR of } f_{q/q}^{(0)[1]}(x) = -\frac{\alpha_s}{2\pi} C_F \frac{1}{\varepsilon}(1-x)$$

$$\boxed{P_{qq}^{[1]}(z) = -\varepsilon Z_{qq}^{[1]}(x) = \frac{\alpha_s}{2\pi} C_F (1-x)}$$

Calculation of DGLAP evolution kernel at one loop

- P_{qq}: Need to calculate $f_{q/q}^{0[1]}$

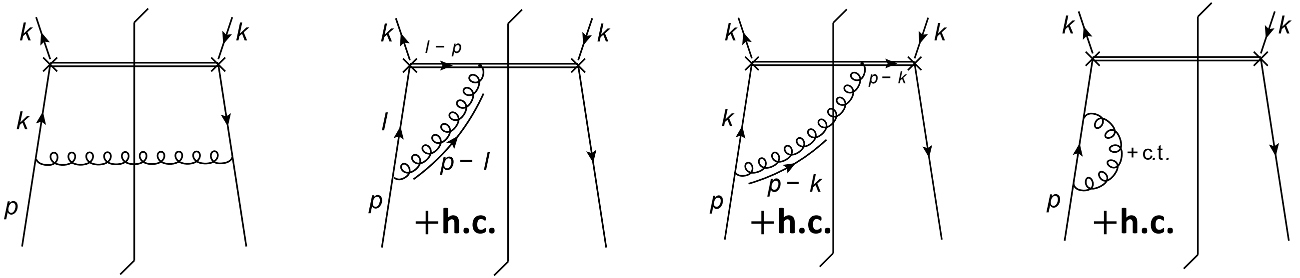

- P_{qq}: Sum over all the diagrams

$$P_{qq}^{[1]}(z) = C_F \left[\frac{2}{(1-z)_+} - 1 - z + \frac{3}{2}\delta(1-z) \right]$$

$$[P(x)]_+ = P(x) \text{ when } 0 < x < 1$$

$$\int_0^1 \mathrm{d}x \, [P(x)]_+ \, f(x) \equiv \int_0^1 dx P(x)(f(x) - f(1))$$

Calculation of DGLAP evolution kernel at one loop

The other kernels

$$P_{qg}^{[1]}(z) = T_F \left[z^2 + (1-z)^2\right]$$

$$P_{gq}^{[1]}(z) = C_F \left[\frac{1+(1-z)^2}{z}\right]$$

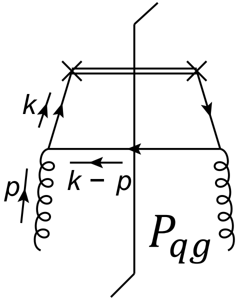

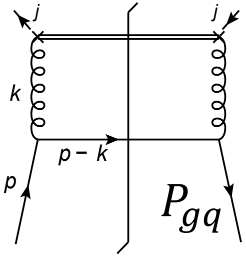

$$P_{gg}^{[1]}(z) = 2C_A \left(\frac{z}{(1-z)_+} + z(1-z) + \frac{1-z}{z}\right) + \left(\frac{11}{6}C_A - \frac{2}{3}n_f T_F\right)\delta(1-z)$$

P_{gg}

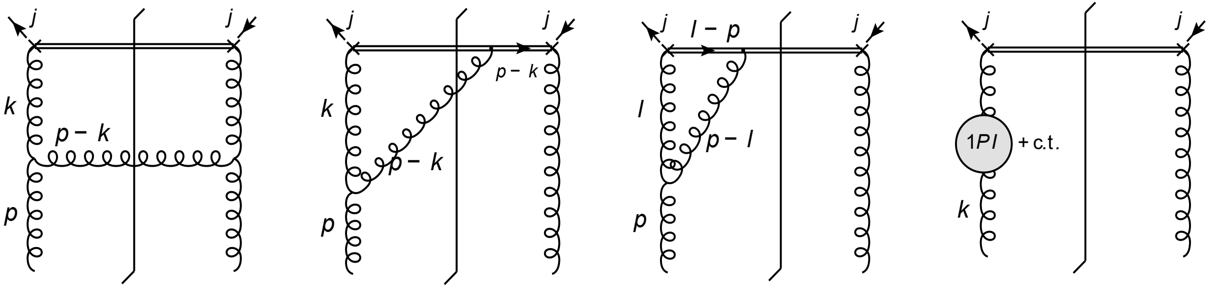

Recitation question

- Why is that gluon and (anti)quark PDFs all grow in the small x region when the energy scale Q becomes larger?
- Why is that the PDF error bands become smaller at high Q scale?

This is a phenomenology of DGLAP equations.

Phenomenology of DGLAP equations

DGLAP evolution

$$\frac{\mathrm{d} f_i(x,\mu)}{\mathrm{d}\ln\mu^2} = \sum_{j=q,\bar{q},g}\int_x^1 \frac{\mathrm{d}z}{z} P_{ij}(x/z, \alpha_s(\mu))\, f_j(z,\mu)$$

Transfers $f(z)$ at $z \in [x, 1]$ to $f(x)$

The large x evolves to small x

Classical picture: successive LO splitting (leading-log evolution)

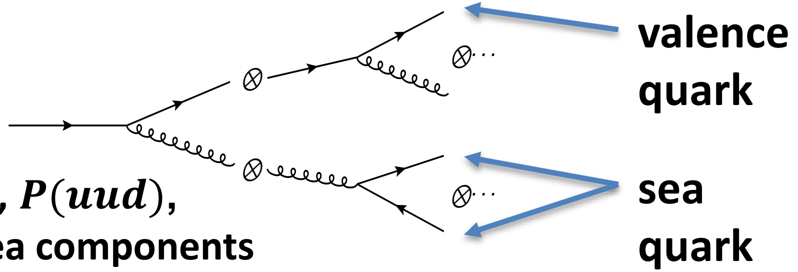

Based on the naïve parton model picture, in a proton, $P(uud)$, constituent quarks (u, d) contain both valence and sea components

$$u_v = u - \bar{u},\quad u_s = \bar{u},\quad d_v = d - \bar{d},\quad d_s = \bar{d}$$

Non-constituent quarks are purely sea components

$$s_s = s = \bar{s},\quad c_s = c = \bar{c},\quad b_s = b = \bar{b}$$

Phenomenology of DGLAP equations

LO evolution

- Both $q \to g$ and $g \to g$ splitting contain $1/z$ singularity
  $\Longrightarrow g(x)$ is singularly large at $x \to 0$
- Sea components can be perturbatively generated from $g \to q\bar{q}$ splitting
  $\Longrightarrow$ sea quark PDFs become large as $x \to 0$
- Since u, d also contain sea components
  $\Longrightarrow$ all the PDFs: $u, d, s, c, \bar{u}, \bar{d}, \bar{s}, \bar{c}$, g … grow as $x \to 0$

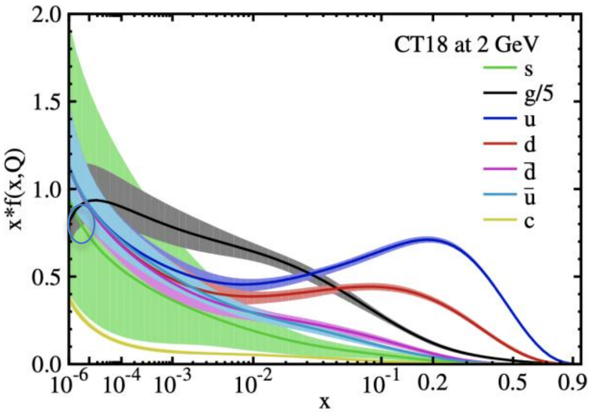

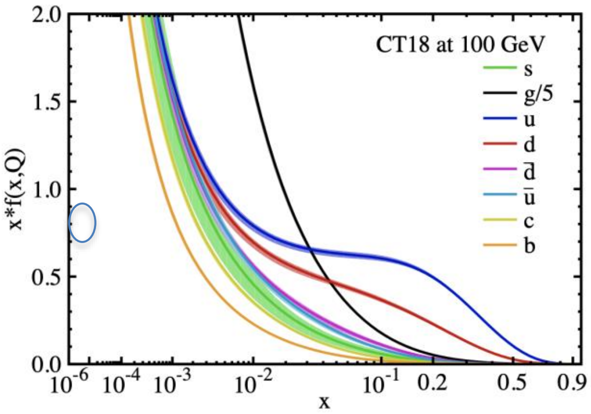

Large x evolves to small x

Perturbative PDF contribution dominates at large scale, so that the PDF error bands become smaller.

PDF uncertainties vary as Q via DGLAP evolution

arXiv: 1912.10053

CT18 NNLO PDFs

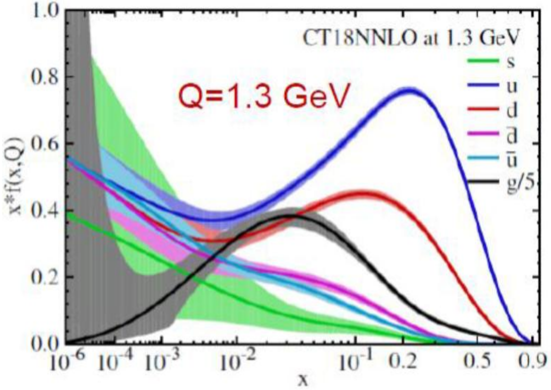

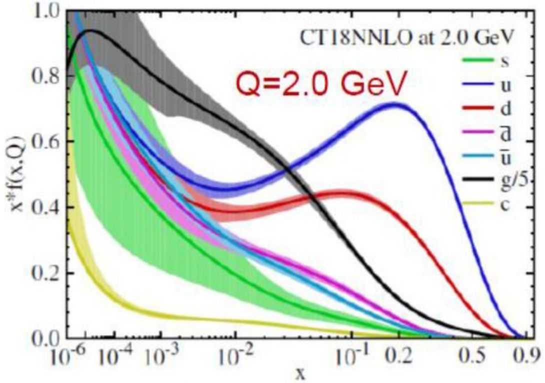

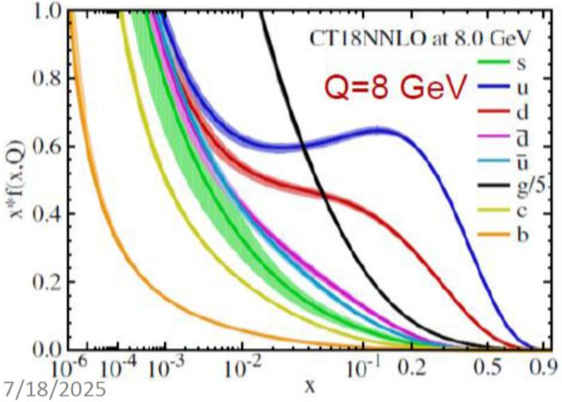

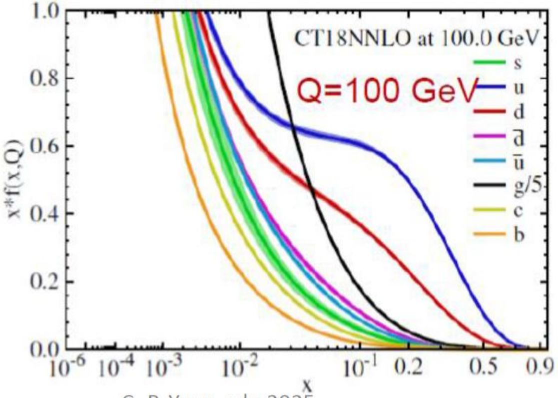

- Faster DGLAP evolution at low Q values.
- Smaller PDF error bands at higher Q values.
- At high Q, perturbaive contribution becomes more important than the non-perturbative part of PDF.

Relatively low energy data, such as HERA I+II, remain crucial for PDF global analysis.

Phenomenology of DGLAP equations

❑ Classical successive splitting picture leads to some wrong impressions

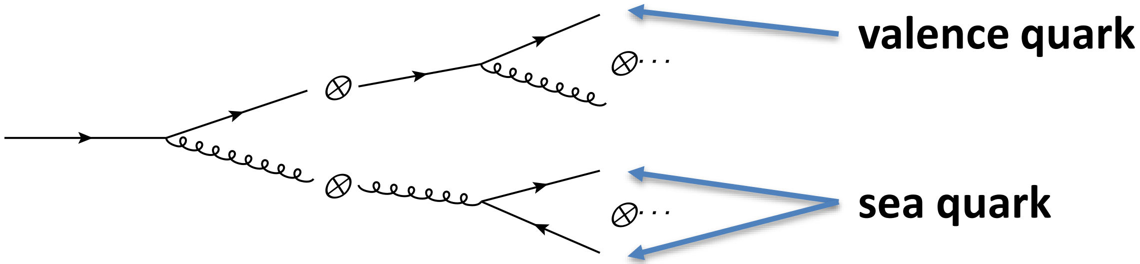

- ➢ $P(u \to \bar{u}) = P(u \to \bar{d})$ (since antiquarks = sea quarks are from gluon splitting)
- ➢ $P(u \to s) = P(u \to \bar{s})$ (since both s and $\bar{s}$ are from gluon splitting

Then based on the naïve parton model picture:

- $P = P(uud)$, only u and d exist at some scale, and
- all the other flavors are from evolution

One would *wrongly* expect

- $\bar{u}(x) = \bar{d}(x) = \bar{s}(x)$
- $s(x) = \bar{s}(x), c(x) = \bar{c}(x), b(x) = \bar{b}(x)$

Broken by higher-order *quantum interference* effects!

Recitation question

- **Assume s$(x) = \bar{s}(x)$ at a very low scale, of the order $\Lambda_{QCD} \sim 300\ MeV$, can perturbative QCD contribution yields s$(x) \neq \bar{s}(x)$ at a large scale Q?**

This is a phenomenology of DGLAP equations.

Phenomenology of DGLAP equations

❑ Evolution kernels at NNLO

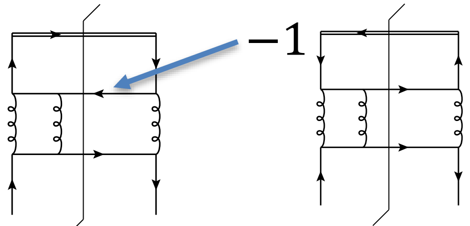

Sea: $q \to q'$ Sea: $q \to \bar{q}'$

$$P_{qq}^s - P_{q\bar{q}}^s \propto -\mathrm{tr}\{t^a t^b t^c\}\,\mathrm{tr}\{t^c t^b t^a\} - \mathrm{tr}\{t^a t^b t^c\}\,\mathrm{tr}\{t^a t^b t^c\} = -\frac{1}{8N_c}\,d_{abc}^2,$$

- **First appears at NNLO**
- **Due to quantum interference**
- **Abelian feature $d^{abc} = 1/4$ for $U(1)$ theory**

❑ Asymmetry between $s(x)$ and $\bar{s}(x)$

can be generated perturbatively

$$\frac{\mathrm{d}}{\mathrm{d}\ln\mu^2}(s-\bar{s}) \supset \left(P_{qq}^s - P_{q\bar{q}}^s\right) \otimes \left(u - \bar{u} + d - \bar{d} + \cdots\right)$$

❖ **Non-zero valence distributions can lead to s-$\bar{s}$ asymmetry**

CT18As

$$s(x) - \bar{s}(x) \neq 0$$

even though $\int_0^1 dx\left(s(x) - \bar{s}(x)\right) = 0$

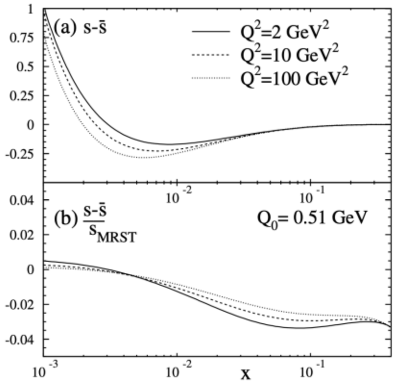

FIG. 2. (a) Strange asymmetry in the nucleon from NNLO QCD evolution for $Q^2 = 2$, 10, and 100 GeV^2; (b) the corresponding ratio to the LO strange density of Ref. [18].

[Catani et.al] hep-ph/0404240

Recitation question

Why is that the integration range of ξ is from Bjorken-x value x_B to 1 in DIS factorization?

Integration range in DIS: why $\xi \in [x_B, 1]$?

$$W^{\mu\nu}(x, Q^2) = \int_{x_B}^{1} \frac{d\xi}{\xi} f(\xi) C^{\mu\nu}(x/\xi, Q^2)$$

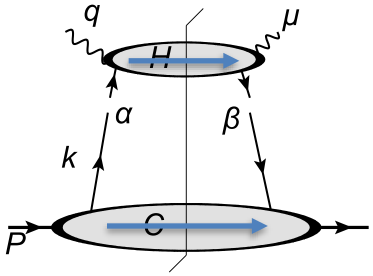

$$P = \left(P^+, \frac{m^2}{2P^+}, 0\right)$$

$$q = \left(-x_B P^+, \frac{Q^2}{2x_B P^+}, 0\right)$$

$$k = (\xi P^+, k^-, \boldsymbol{k}_T)$$

<u>Cut diagram</u>:

- **In H: momentum flowing through the cut**

$$(k+q)^+ = (\xi - x_B)P^+ \geq 0 \Longrightarrow \xi \geq x_B$$

- **In C: momentum flowing through the cut**

$$(P-k)^+ = (1-\xi)P^+ \geq 0 \Longrightarrow \xi \leq 1$$

$$\xi \in [x_B, 1]$$

- **Cut line distinguishes quark and antiquark lines, so all the flavors are summed over, with $\xi \in [x_B, 1]$**

Conclusion of Part I

- QCD Factorization is the rigorous mathematical formalism of the Feynman's parton model from the first principles of QCD.
- It separates hard and low energy scales, and makes use of asymptotic freedom of QCD.
- It provides a clear operator definition for the PDFs, allowing it to be studied by itself within field theory (Lattice QCD).
- It allows an unambiguous procedure for perturbatively calculating the hard parton scattering cross sections, whose convolution with PDFs provides physical predictions.
- It introduces a factorization scale μ to both the PDF and hard scattering coefficients.
- Requiring the physical cross sections to be independent of μ leads to a set of evolution equations, called DGLAP equations.
- The full spin dependence of both the hadron and partons can be consistently included, together with their evolution equations.
- Higher order QCD and electroweak corrections are needed to compare to precision experimental data.

How to use PDFs and their tools

from a user's point of view

Some basics about PDFs: relevant kinematics in (x, Q^2)

C T E Q

Q^2

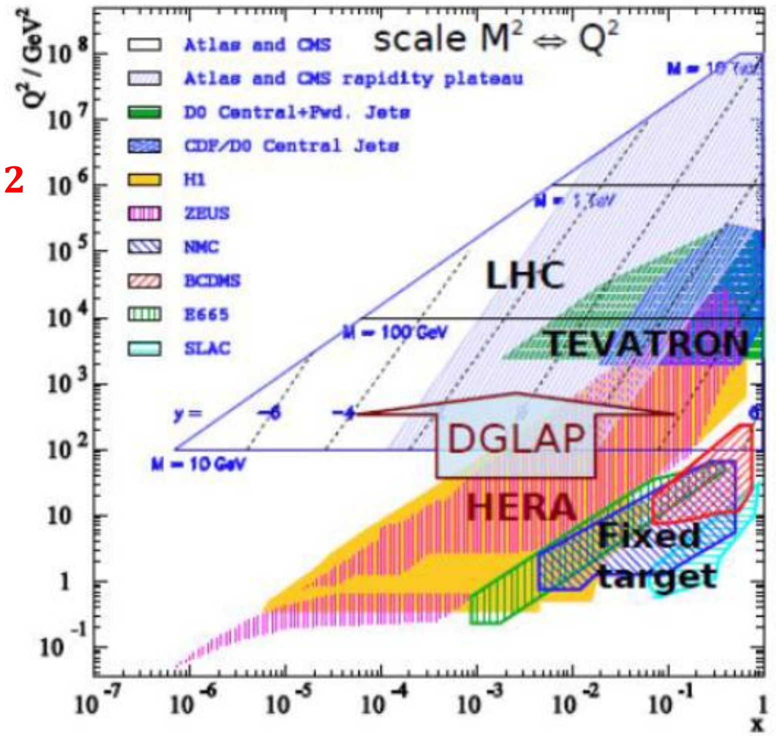

X

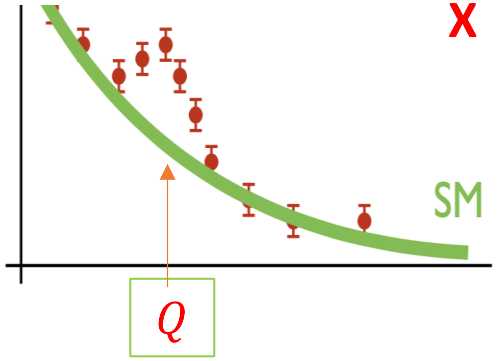

$$\sigma(Q) \simeq \sum_{i,j} f_{i/p}(x_1, Q) \otimes f_{j/p}(x_2, Q) \otimes \hat{\sigma}_{ij}(x_1, x_2; Q)$$

- Parton Distribution Function $f(x, \mathrm{Q})$
- Given a heavy resonance with mass Q produced at hadron collider with c.m. energy $\sqrt{S}$
- What's the typical x value?

$$\langle x \rangle = \frac{Q}{\sqrt{S}}$$ at central rapidity (y=0)

- Generally, $x_1 = \frac{Q}{\sqrt{S}} e^{y}$ *and* $x_2 = \frac{Q}{\sqrt{S}} e^{-y}$

$$x_1 + x_2 = 2\frac{Q}{\sqrt{S}}\cosh(y) \Rightarrow y_{\max} : x_1 + x_2 = 1$$

PDF uncertainties vary as Q via DGLAP evolution

arXiv: 1912.10053

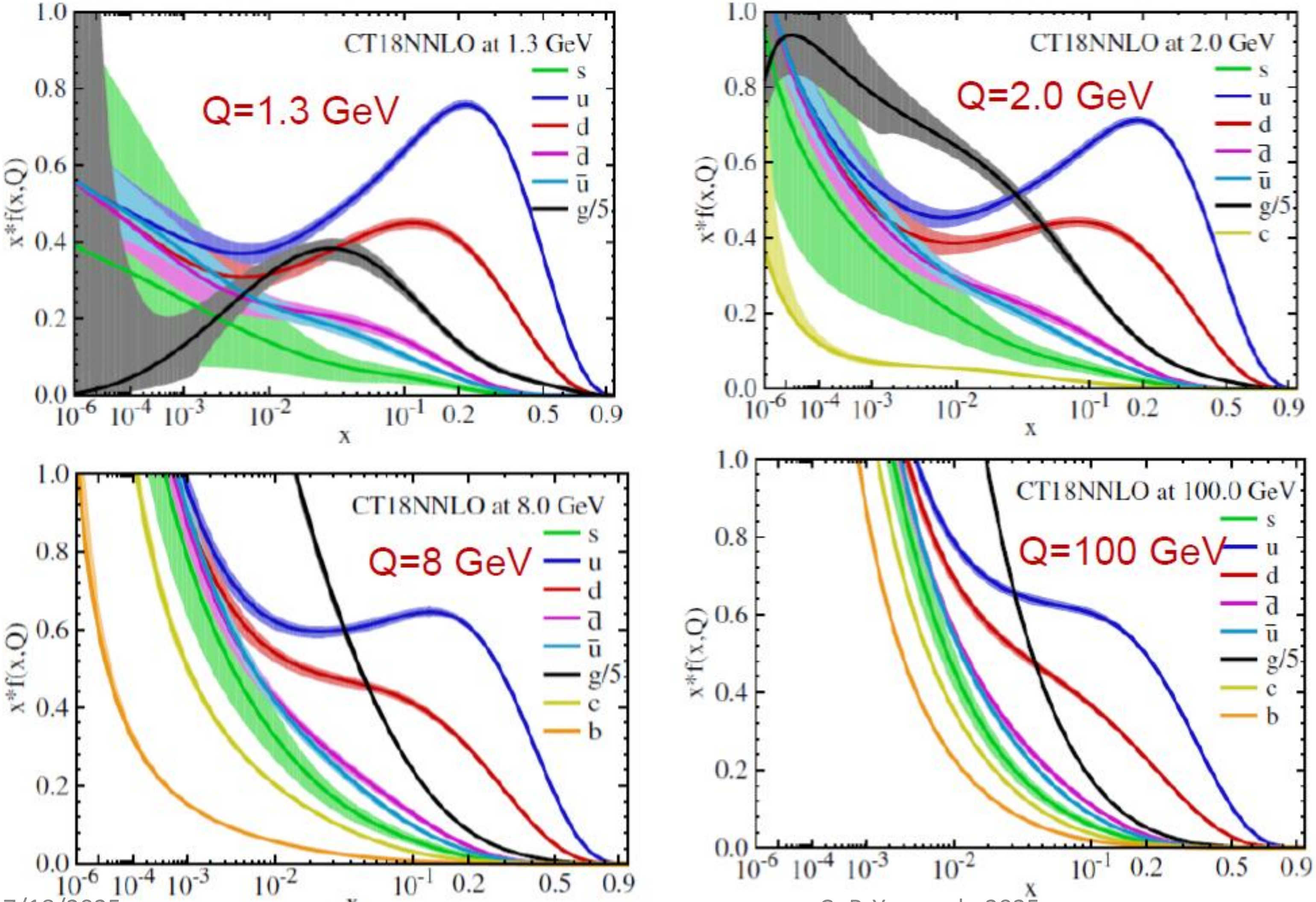

CT18 NNLO PDFs

- Faster DGLAP evolution at low Q values.
- Smaller PDF error bands at higher Q values.
- At high Q, perturbaive contribution becomes more important than the non-perturbative part of PDF.

Relatively low energy data, such as HERA I+II, remain crucial for PDF global analysis.

Momentum fractions inside proton

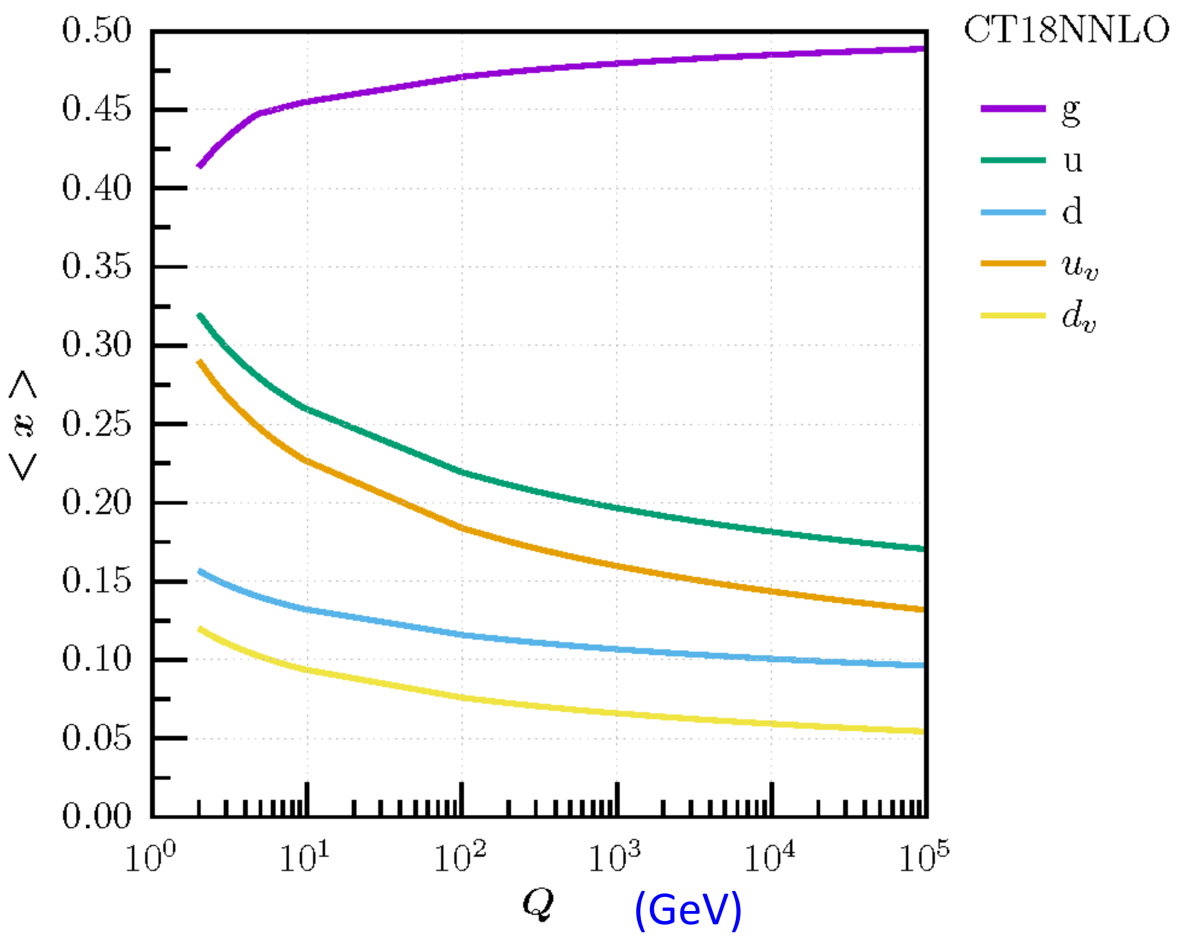

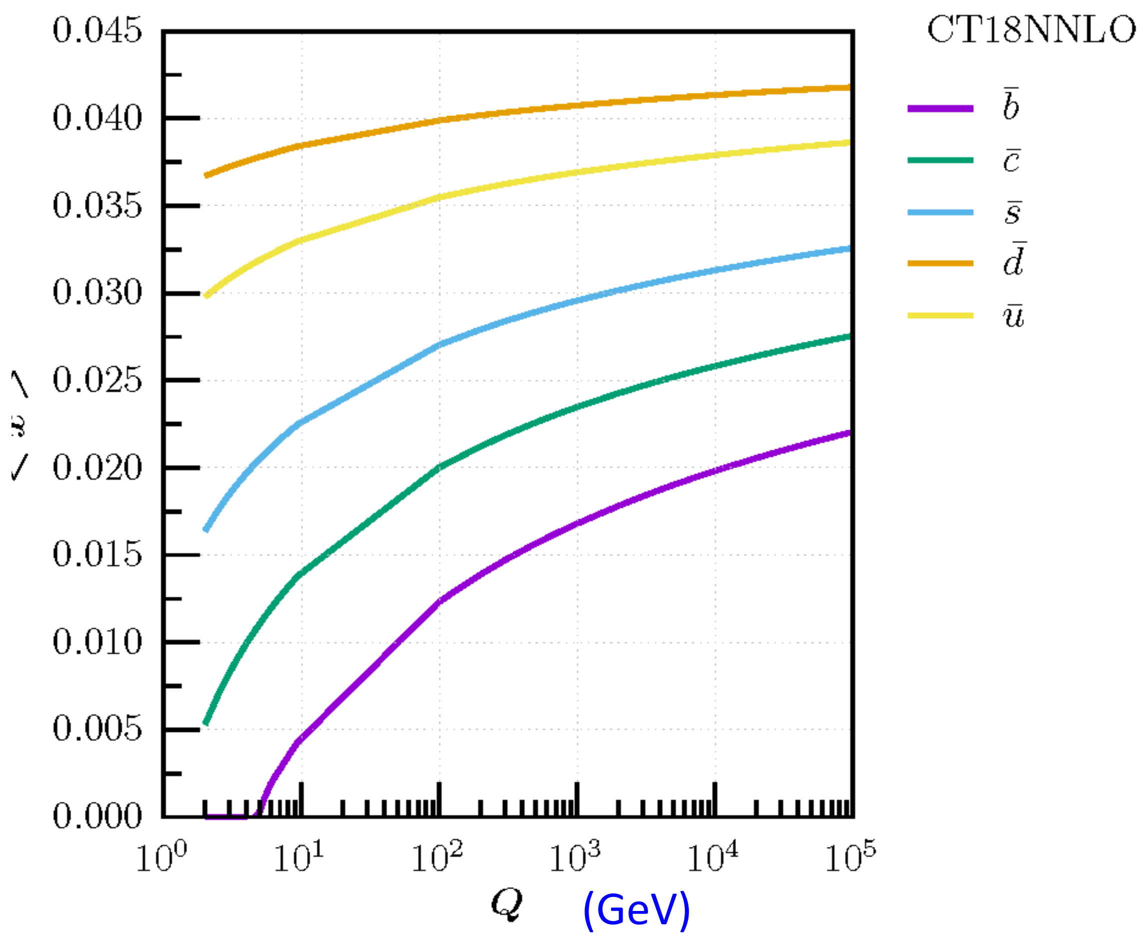

CT18 PDFs and their uncertainties

C T E Q

arXiv:1912.10053

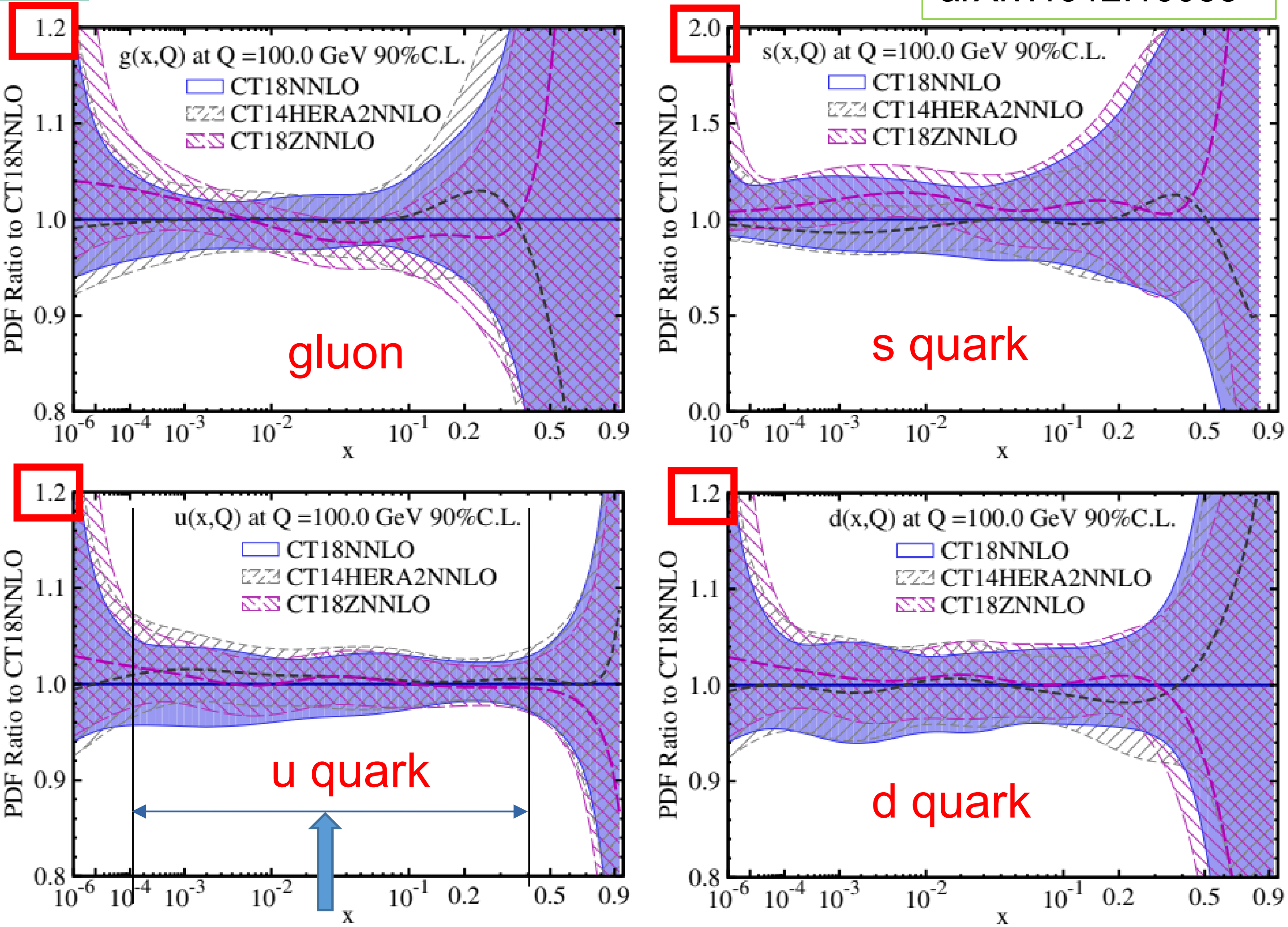

Better constrained by precision experimental data

- PDFs are better determined at $10^{-4} < x < 0.4$
- Regions of x→1 and x→0 are not experimentally accessible; could use lattice QCD predictions at large x
- Large uncertainty for strangeness PDF, especially in large x region.

Using Hessian method:

$$\delta^+ X = \sqrt{\sum_{i=1}^{N_a} \left[\max\left(X_i^{(+)} - X_0, X_i^{(-)} - X_0, 0\right)\right]^2},$$

$$\delta^- X = \sqrt{\sum_{i=1}^{N_a} \left[\max\left(X_0 - X_i^{(+)}, X_0 - X_i^{(-)}, 0\right)\right]^2},$$

For CT18, $N_a = 29$

QCD Global analysis of PDFs

Based on QCD Factorization formalism

Global analysis of PDFs

- PDFs are usually extracted from global analysis on variety of data, e.g., DIS, Drell-Yan, jets and top quark productions at fixed-target and collider experiments, with increasing weight from LHC, together with SM QCD parameters [see 1709.04922, 1905.06957 for recent review articles]

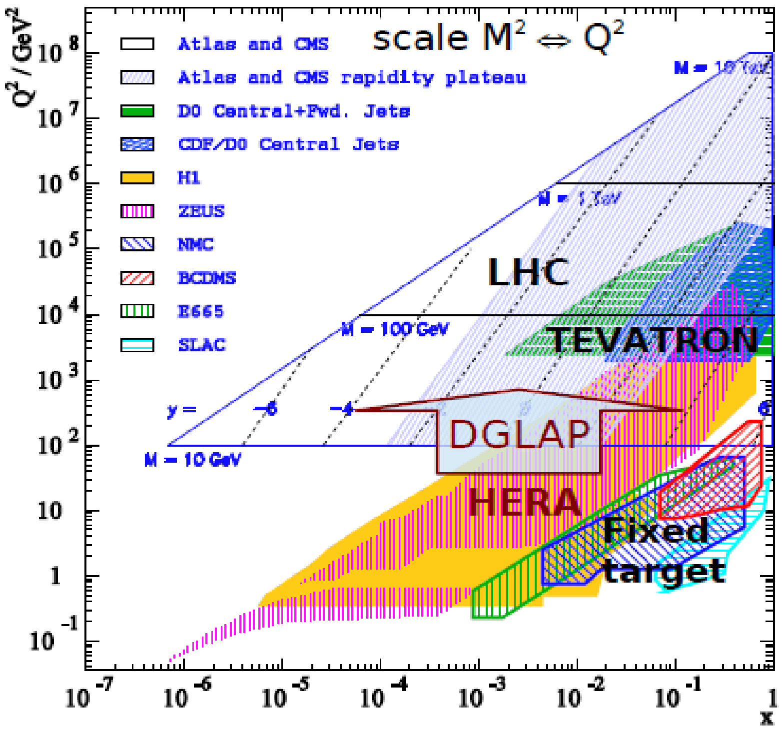

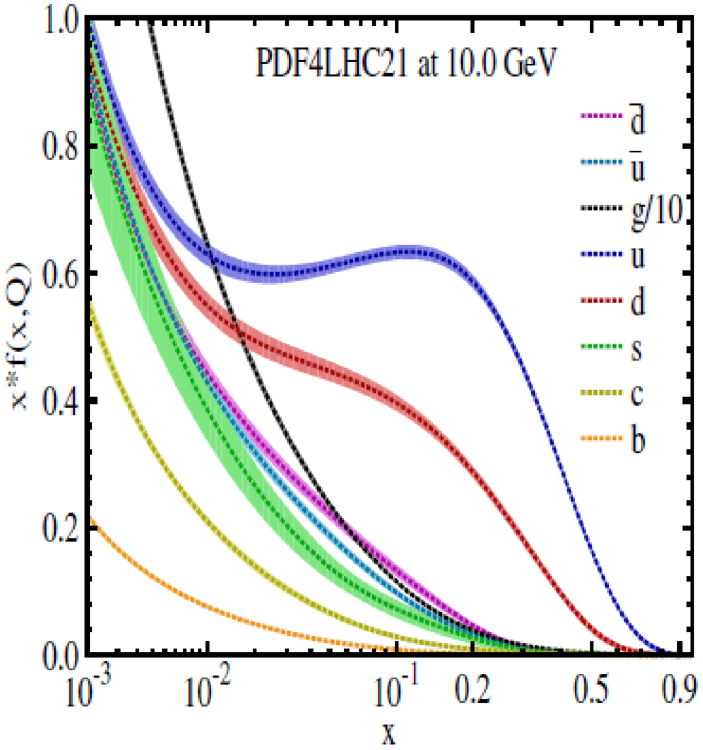

parameter variations

$\alpha_S(M_Z)$

Mc, Mb, Mt

QCD/EW corrections

nuclear corrections

EW parameters

New Physics

- diversity of the analysed data are important to ensure flavor separation and to avoid theoretical/experimental bias; possible extensions to include EW parameters and possible new physics for a self-consistent determination

- alternative approach from lattice QCD simulations, for various PDF moments or PDFs directly calculated in x-space with large momentum effective theory or pseudo-PDFs [2004.03543]

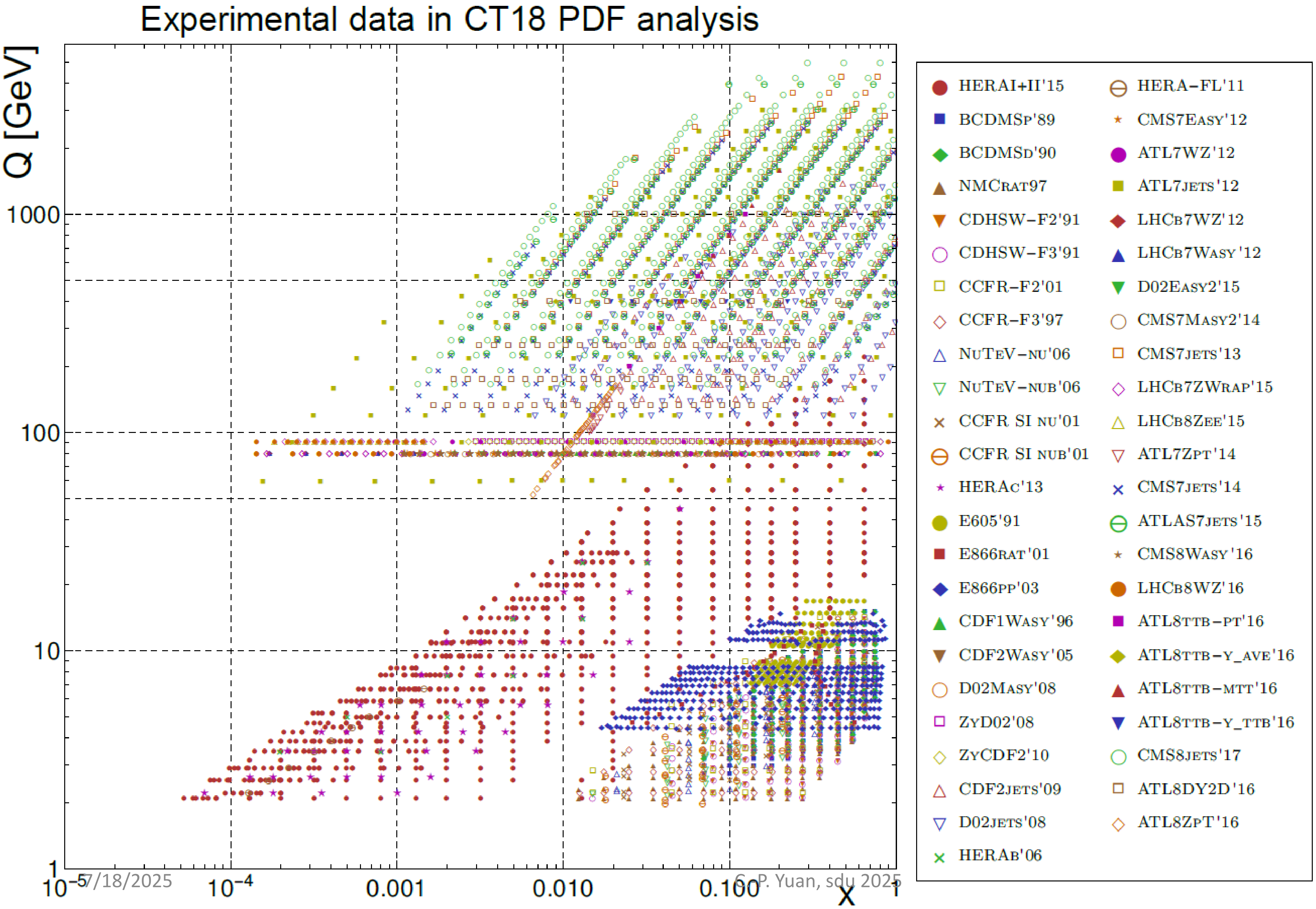

arXiv: 1912.10053

Comparing predictions from various QCD global analysis groups

Snowmass 2021, 2203.13923

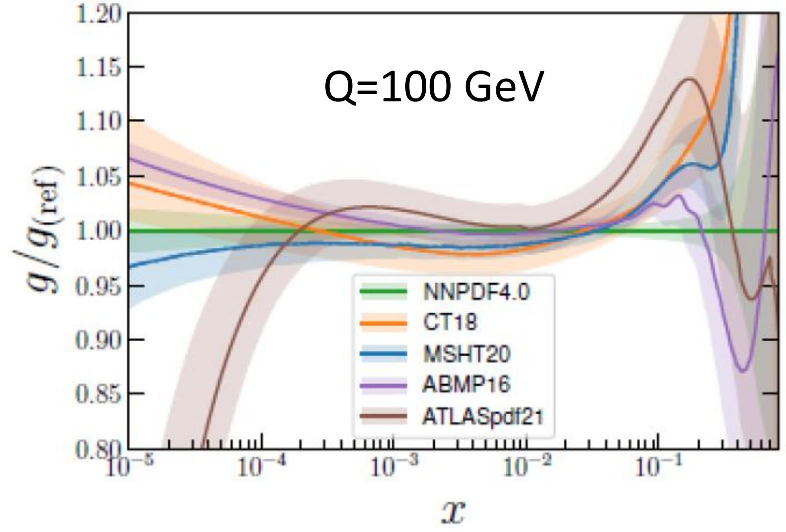

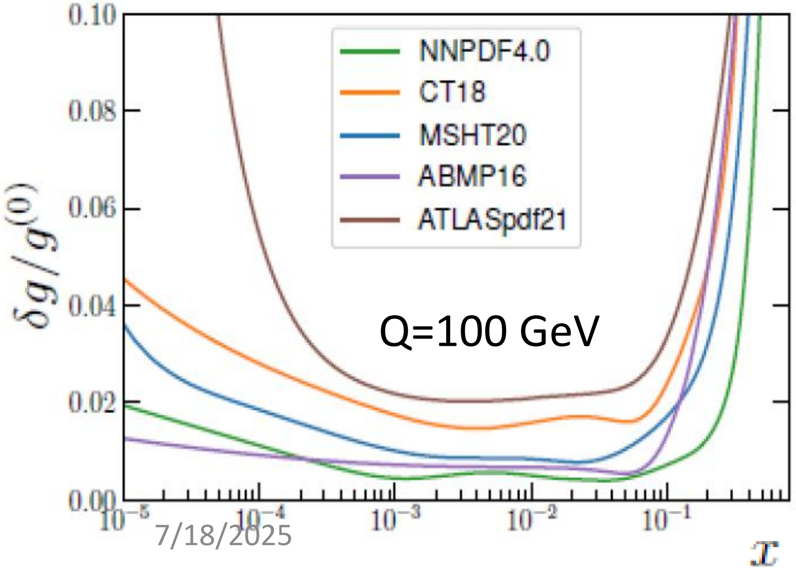

Smaller PDF errors lead to smaller

PDF luminosity errors, then smaller PDF-induced errors in cross sections.

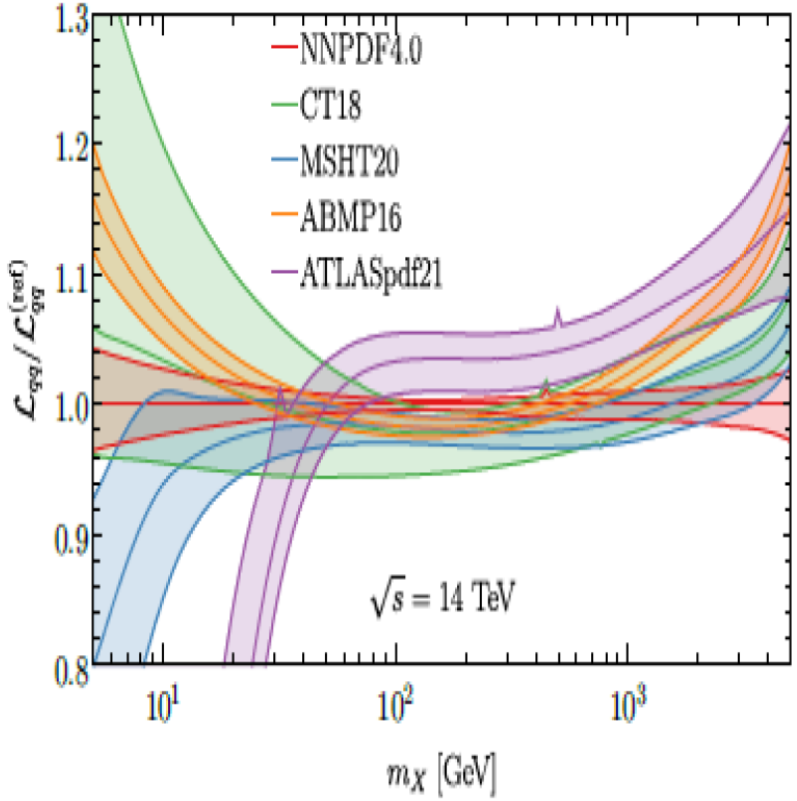

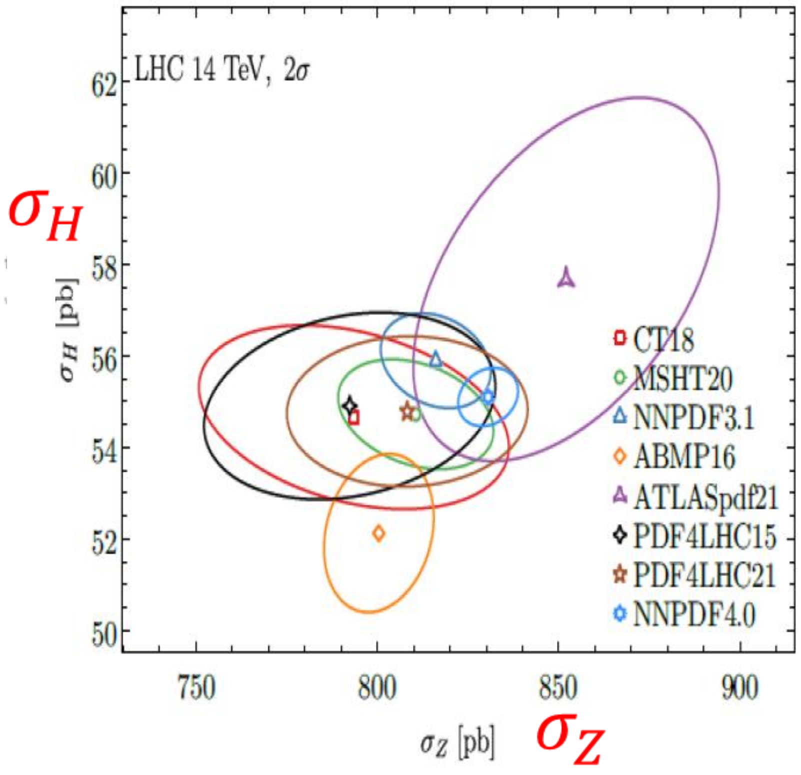

Comparing predictions from various QCD global analysis groups

C T E Q

Snowmass 2021, 2203.13923

The PDF-induced errors @ 68% CL in
$gg \to h$ and $q\,\bar{q} \to Z$ NNLO cross sections

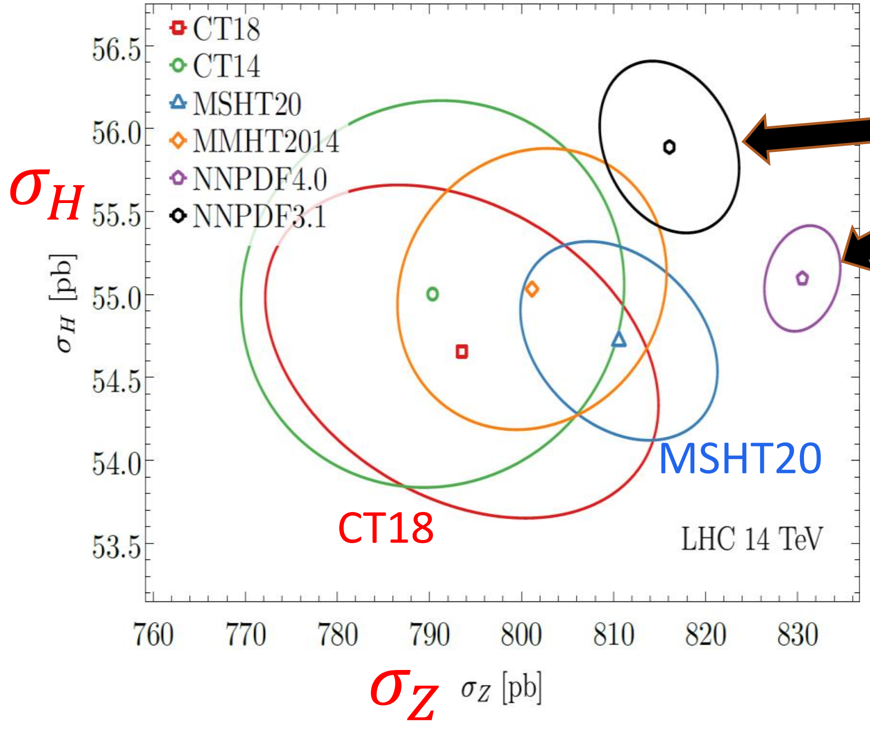

NNPDF3.1

NNPDF4.0

Their predictions do not overlap at 1σ level.

Different (though mostly consistent) predictions on

- central values and error estimates of PDFs,
- parton luminosities,
- physical cross sections, and
- various correlations among PDFs and data …

Due to different choices of

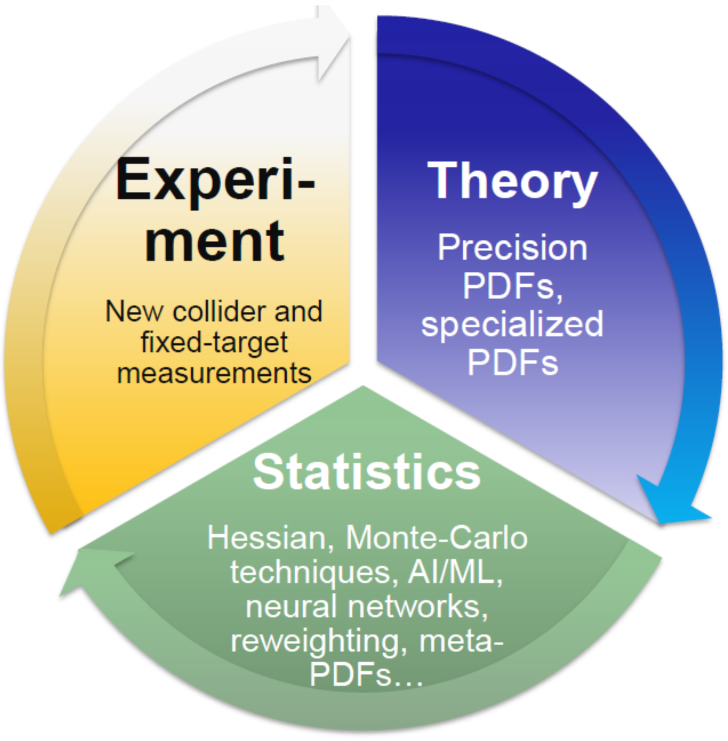

Components of a global QCD fit

Benchmark Study: PDF4LHC21

arXiv:2203.05506

Relative PDF uncertainties on the gg luminosity at 14 TeV in three PDF4LHC21 fits to the **identical** reduced global data set

arXiv:2203.05506

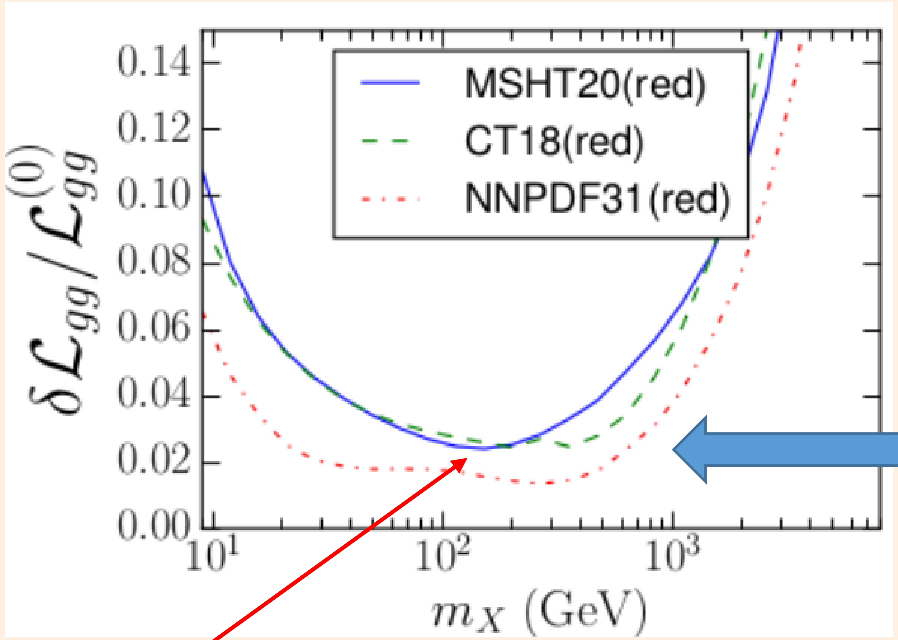

$\times$ 1.5 – 2 difference

- Each analysis group (CT, MSHT, NNPDF) used the same (reduced) data sets and same theory predictions in the analysis

Smaller error size found by NNPDF

- NNPDF3.1' and especially 4.0 (based on the NN's+ MC technique) tend to give smaller uncertainties in data-constrained regions

The size of PDF error estimates depends on the methodology of global analysis adopted by the PDF fitting group.

Sources of PDF errors

Factorization Theorem:

Data = PDFs $\otimes$ Hard part cross sections (Wilson coeff.)

Experimental errors:

- Statistical
- Systematic
- uncorrelated
- correlated
- χ^2definition (experimental or t_0)
- Possible tensions among data sets

Extracted with errors, dependent of methodology of analysis

- Non-perturbative parametrization forms of PDFs
- Additional theory prior
- Choice of Tolerance (T^2) value

Theoretical errors:

- Which order: (NLO, NNLO, …, resummation – BFKL, qT, threshold)
- Which scale: (μ_F, μ_R)
- Which code: (antenna subtraction, sector decomposition,…, qT, N-jettiness,,…)
- Monte Carlo error: (most efficient implementation,…)

How to estimate PDF errors in QCD global analysis

- Error estimate is important.
- Two different methodology in global analysis

❖ Hessian PDF eigenvector (EV) sets,
from analytic parametrizations of PDFs
➡ (ABM, CTEQ, HERA, MSHT, …)

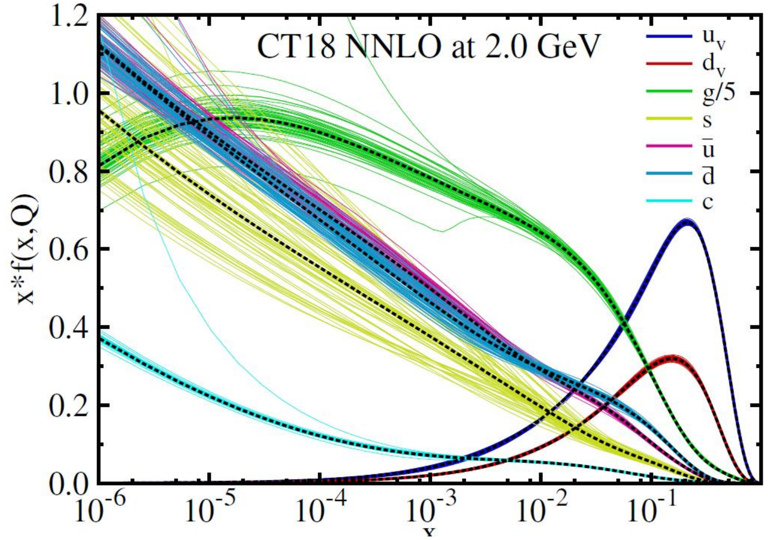

❖ Monte Carlo (MC) PDF replicas,
from Neural Network (NN) parametrizations
➡ (NNPDF)

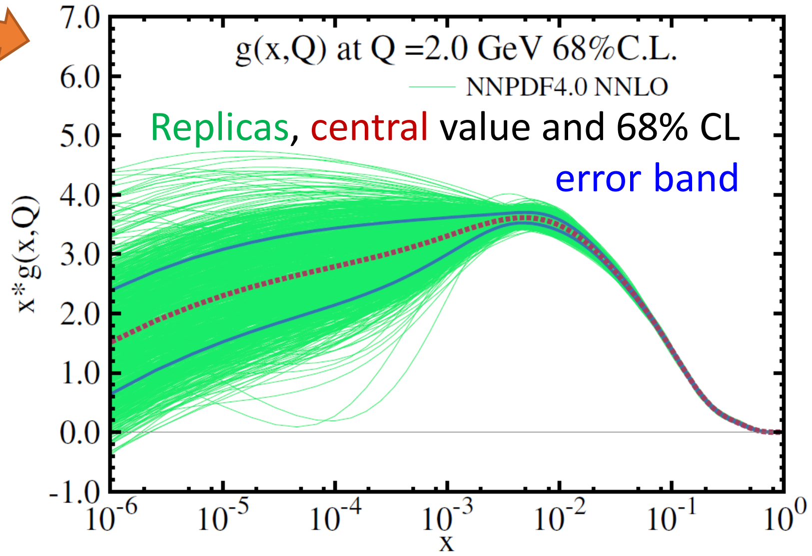

- Both methods assume some non-perturbative input of PDFs at the initial Q_0 scale, around 1 GeV. (analytical parametrization vs. NN architecture)

- They are two powerful and complementary representations.
- Hessian PDFs can be converted into MC ones, and vice versa.

How to quantify PDF uncertainties

was first introduced in 2001 by

Jon Pumplin, Dan Stump and Wu-Ki Tung

@ Michigan State University

hep-ph/0101032

Uncertainties of predictions from PDFs:

The Hessian method

hep-ph/0101051

Uncertainties of predictions from PDFs:

The Lagrange multiplier method

$$\chi^2 = \chi_0^2 + \sum_{i,j} H_{ij}\,(a_i - a_i^0)\,(a_j - a_j^0)$$

It was first implemented in CTQE6 PDFs.

They were used to determine uncertainty of PDFs, physical cross sections, α_s and m_t as well as exploring tensions among data sets in the CTEQ-TEA analysis.

Lagrange Multiplier scan

To explore PDF-induced errors in the determination of $\alpha_s(M_Z)$ and tensions among data sets included in the fit

arXiv:1912.10053

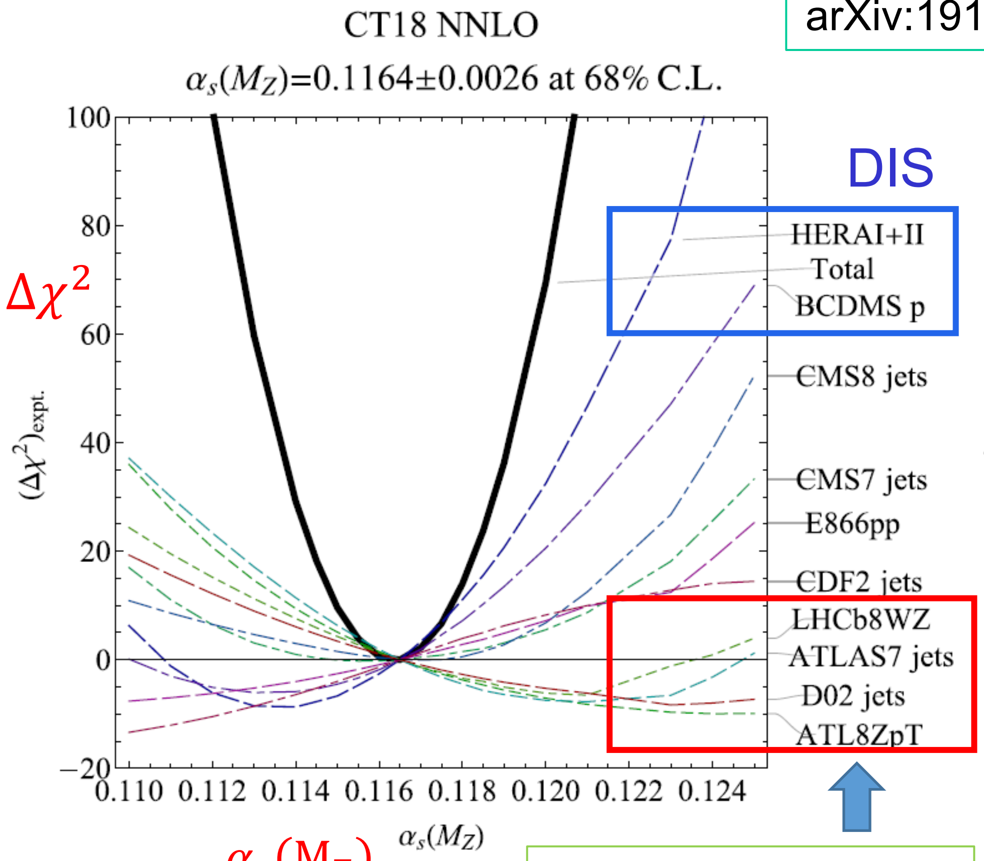

Prefer larger $\alpha_s(M_Z)$

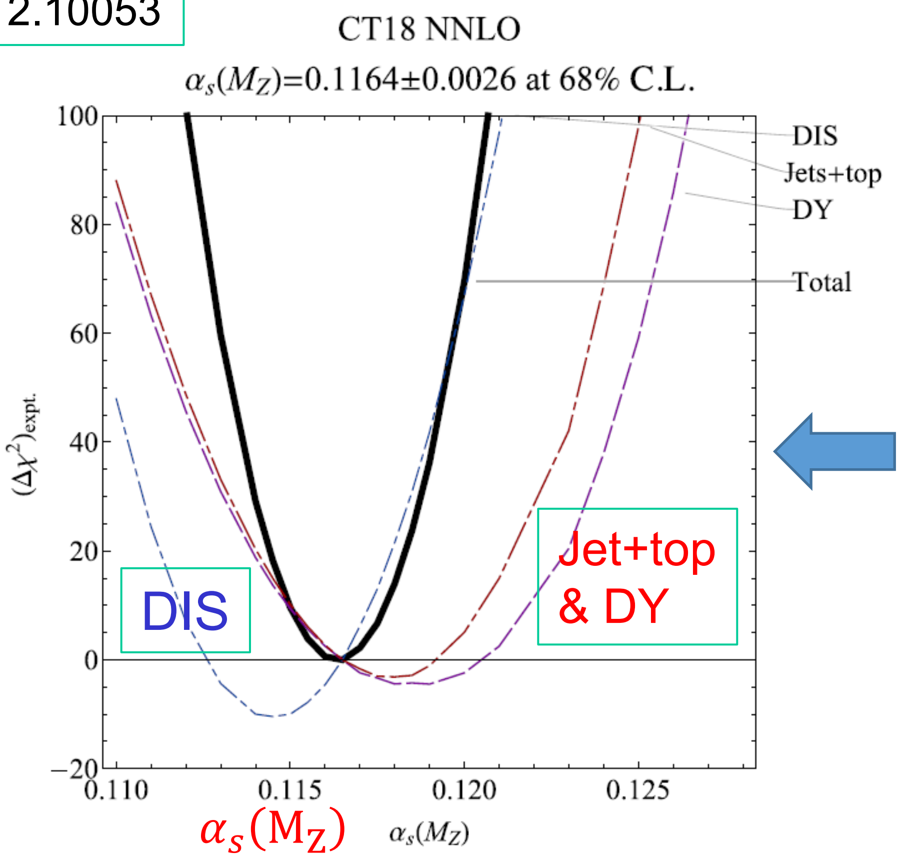

The scan of $\alpha_s(M_Z)$ values in CT18 NNLO PDF analysis.

- The opposing pulls (i.e., tensions) of DIS and jet+top&DY experiments significantly exceed $\Delta\chi^2 = 1$ variation, as implied by the simplest statistical framework.
- Require a large value of Tolerance T^2, the maximum allowed total $\Delta\chi^2$, with $\Delta\chi^2 > 1$
- To agree with the error in $\alpha_s(M_Z)$, 0.007, as provided by PDG (in 2010), without including hadron collider data in the fit, it requires

$$1 < \Delta\chi^2 \le (5-10)$$

Possible tensions among experimental data sets

Require $\Delta\chi^2 > 1$

Tensions among experimental data sets

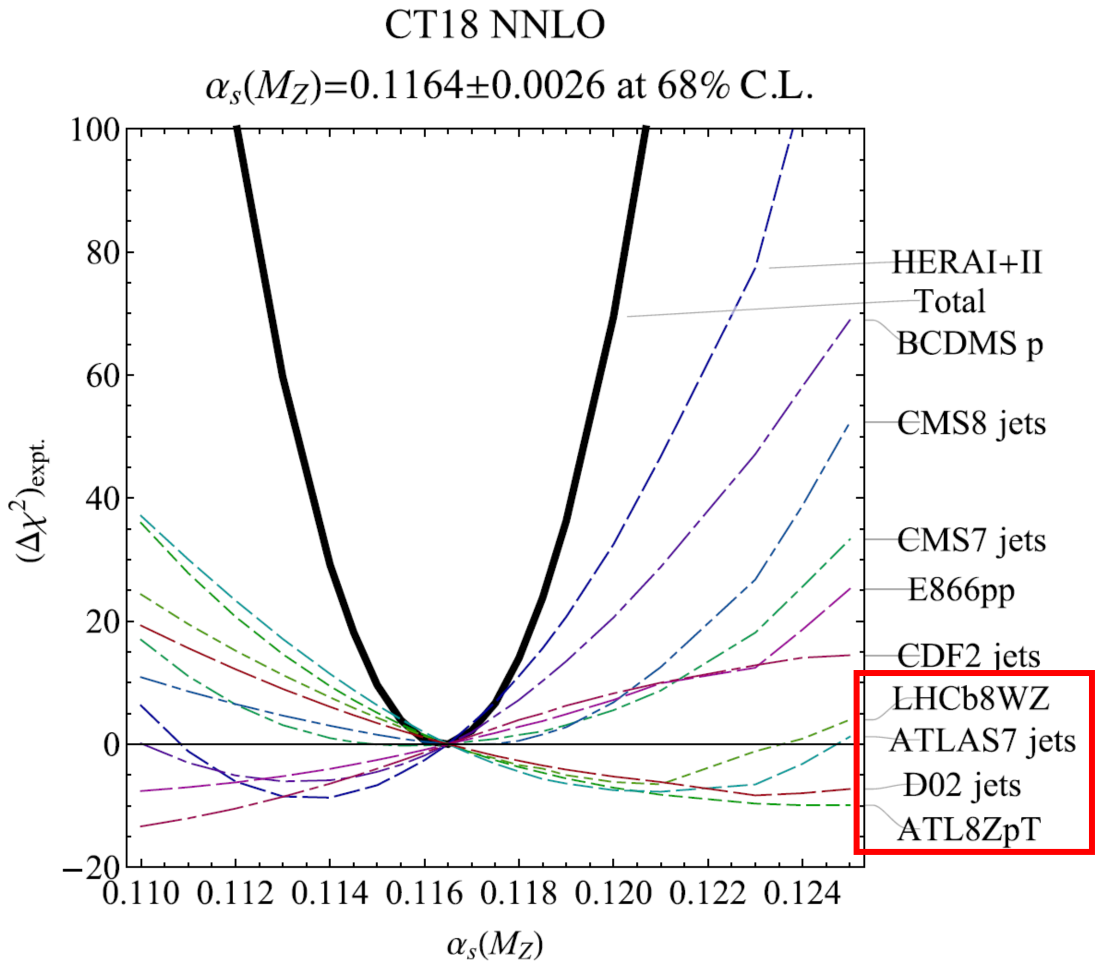

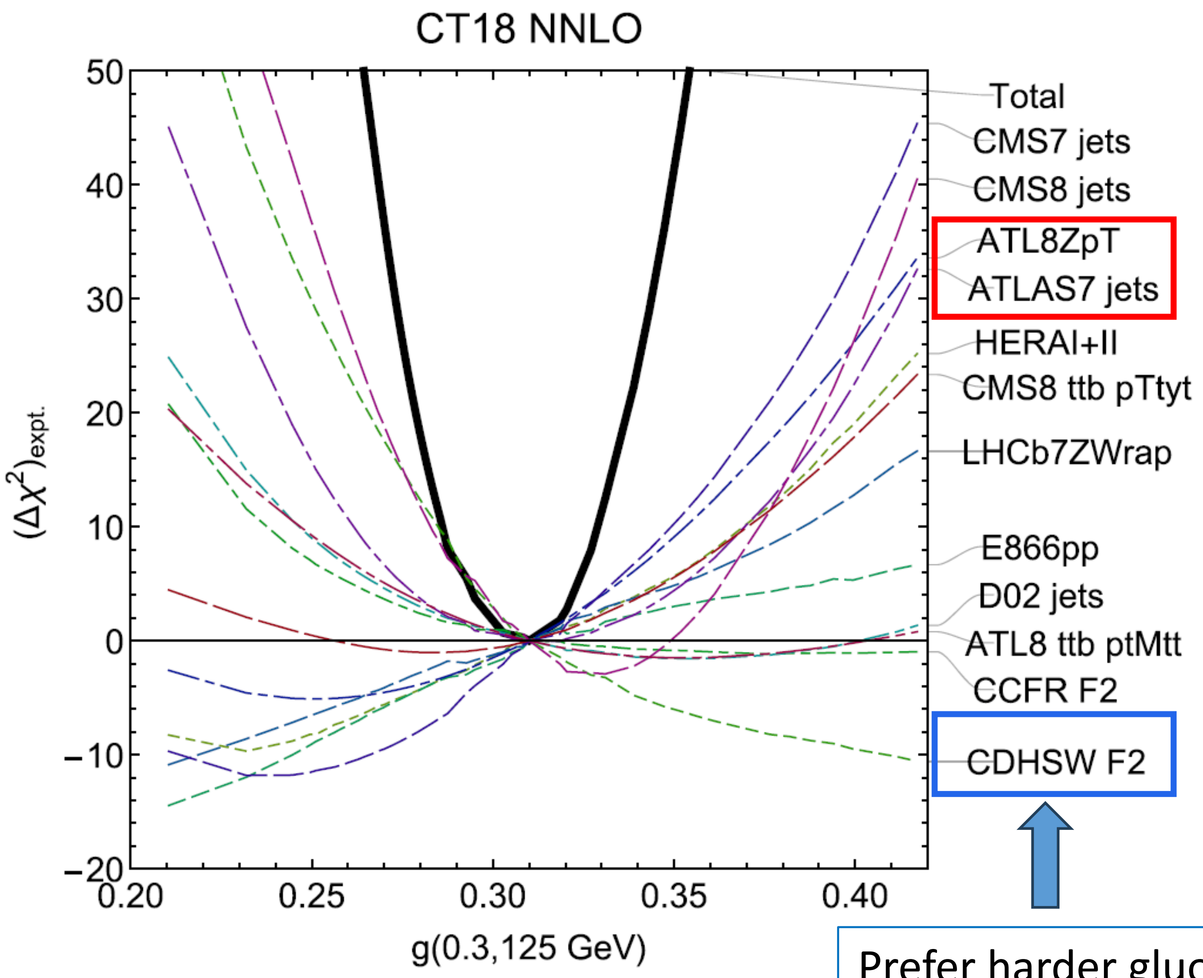

Prefer harder gluon PDF at large x.

Tolerance (T^2) values in various PDF analysis groups

CTEQ

- Tolerance T^2, the maximum allowed total $\Delta\chi^2$ value away from the best (or central) fit, was introduced to account for the sampling of
  - non-perturbative parametrization of PDFs (or NN architecture, smoothness, positivity) and
  - the allowed PDF variation due to various choices of data sets and theory calculations, etc.

- Roughly speaking, at the 68% CL,
  - CTEQ-TEA (CT) Tier-1 $T^2 \sim 30$
  - MSHT dynamical $T^2 \sim 10$
  - NNPDF effective $T^2 \sim 2$ (for MC replicas and their Hessian representation)

- A smaller T^2 value typically yields a smaller PDF error estimate.

CT tolerance includes both Tier-1 and Tier-2 contributions.

To reduce PDF uncertainty, one must maximize both

PDF fitting accuracy
(accuracy of experimental, theoretical and other inputs)

and

PDF sampling accuracy
(adequacy of sampling in space of possible solutions)

Compare PDF error bands with T = 37 or 10 (of CT18) and MSHT20, at 68% CL

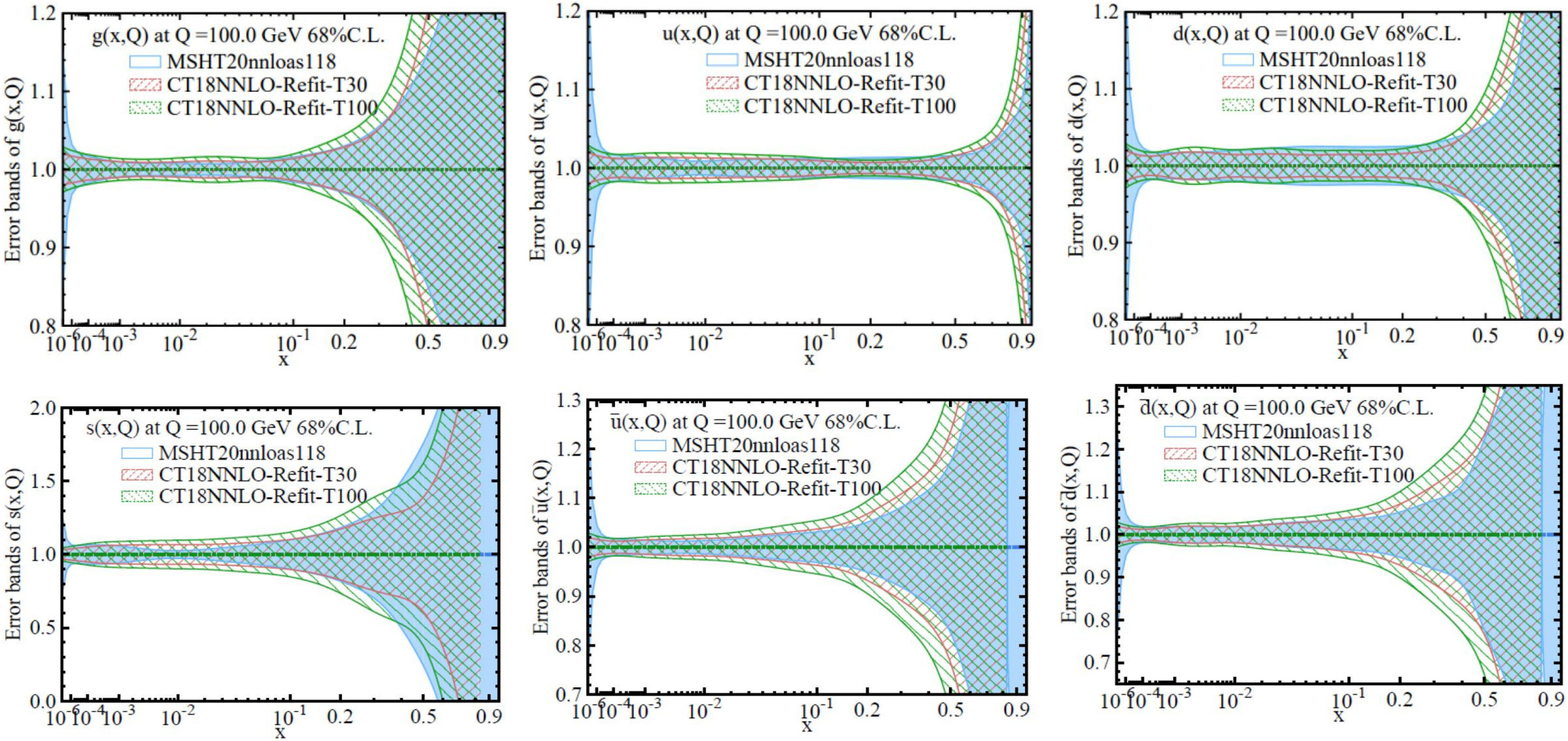

The PDF errors of MSHT20 and CT18 (T=10) are alike in many cases.

26

Hessian profiling of CT and MSHT PDFs cannot use $\Delta\chi^2 = 1$

C T E Q

ATLAS-CONF-2023-015

The statistical analysis for the determination of $\alpha_s(m_Z)$ is performed with the xFitter framework [60]. The value of $\alpha_s(m_Z)$ is determined by minimising a χ^2 function which includes both the experimental uncertainties and the theoretical uncertainties arising from PDF variations:

$$\chi^2(\beta_{\rm exp}, \beta_{\rm th}) = \sum_{i=1}^{N_{\rm data}} \frac{\left(\sigma_i^{\rm exp} + \sum_j \Gamma_{ij}^{\rm exp}\beta_{j,\rm exp} - \sigma_i^{\rm th} - \sum_k \Gamma_{ik}^{\rm th}\beta_{k,\rm th}\right)^2}{\Delta_i^2} + \sum_j \beta_{j,\rm exp}^2 + \sum_k \beta_{k,\rm th}^2 .$$

profiling of CT and MSHT PDFs requires to include a tolerance factor $T^2 > 10$ as in the ePump code

arXiv: 1907.12177

arXiv:1912.10053

- xFitter profiling uses $\Delta\chi^2 = 1$, by default.
- For CT (or MSHT) PDFs, using $\Delta\chi^2 = 1$ in profiling is equivalent to assigning a weight of about 30 (or 10) to the new data included in the fit. Hence, it will overestimate the impact of new data.
- CT: $T^2 \sim 30$; MSHT: $T^2 \sim 10$

When profiling a new experiment with the prior imposed on PDF nuisance parameters $\lambda_{\alpha,th}$:

$$\chi^2(\vec{\lambda}_{\rm exp}, \vec{\lambda}_{\rm th}) = \underbrace{\sum_{i=1}^{N_{pt}} \frac{\left[D_i + \sum_\alpha \beta_{i,\alpha}^{\rm exp}\lambda_{\alpha,\rm exp} - T_i - \sum_\alpha \beta_{i,\alpha}^{\rm th}\lambda_{\alpha,\rm th}\right]^2}{s_i^2}}_{\text{new experiment}} + \underbrace{\sum_\alpha \lambda_{\alpha,\rm exp}^2 + \sum_\alpha T^2\lambda_{\alpha,\rm th}^2}_{\text{priors on expt. systematics and PDF params}} .$$

$$\beta_{i,\alpha}^{\rm th} = \frac{T_i(f_\alpha^+) - T_i(f_\alpha^-)}{2},$$

Impact of higher order theoretical predictions

- Theoretical errors can be larger than experimental errors, even at the NNLO in QCD interaction.

Different (NNLO) theory predictions from various codes; require $\Delta\chi^2 > 1$

arXiv:1912.10053

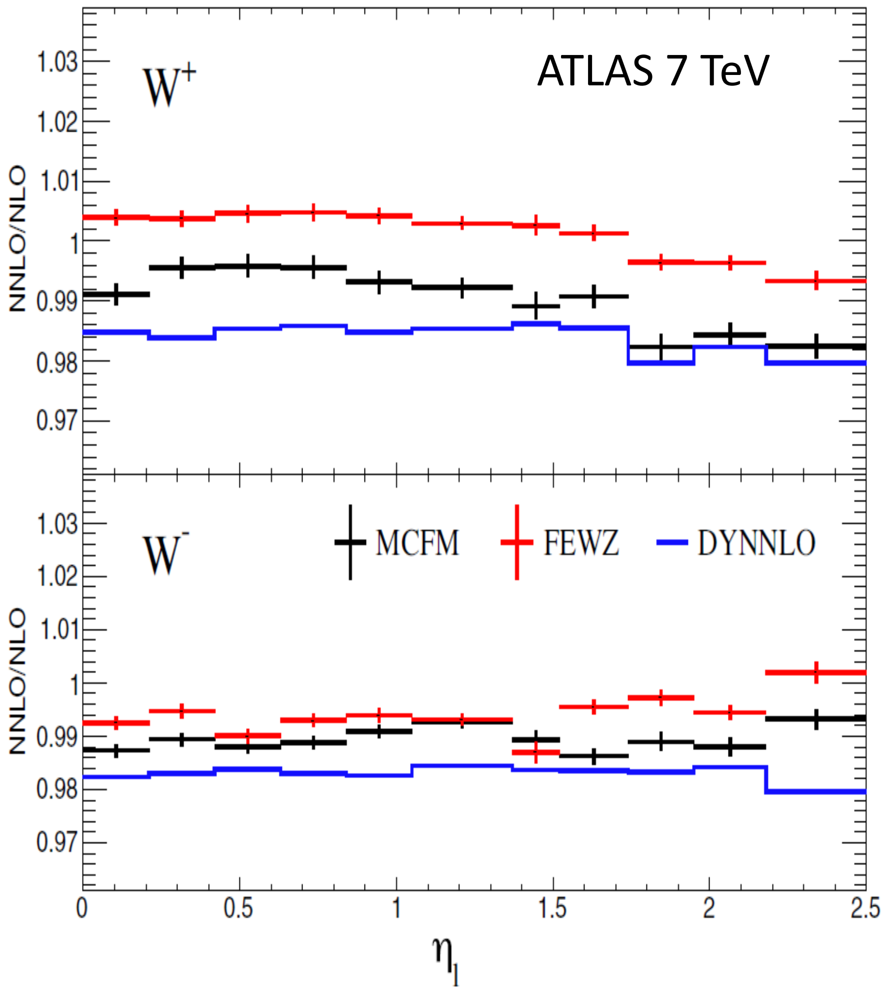

- Compare predictions of three different codes:
  - FEWZ (sector decomposition)
  - MCFM (N-jettiness)
  - DYNNLO (qT)
- Their predictions agree well at NLO.
- Their NNLO predictions agree well for inclusive cross sections (without imposing kinematic cuts).
- Their NNLO predictions for fiducial cross sections (with kinematic cuts) can differ at percent level, while the statistical error of the data is at the sub-percent level.

✓ The resulting PDFs from various theory predictions only differ slightly, when including this data in the CT18A fit.

✓ The kind of theory uncertainty is accounted for by choosing a larger Tolerance value than 1 (i.e., $\Delta\chi^2 > 1$) at the 68% CL.

Missing higher order (MHO) uncertainty estimated by scale variation

- General wisdom: Varying a “typical scale” by a factor of 2 (or 7-point scales) to estimate missing higher order (MHO) contribution.
- This wisdom does not always work. Namely, varying the factorization and normalization scales by a factor of 2 cannot accurately estimate MHO contribution.

The complete higher order calculations in QCD, EW, and the mixed QCD+EW are all very important for making precision theory prediction to compare to precision experimental data in order to extract precision PDFs.

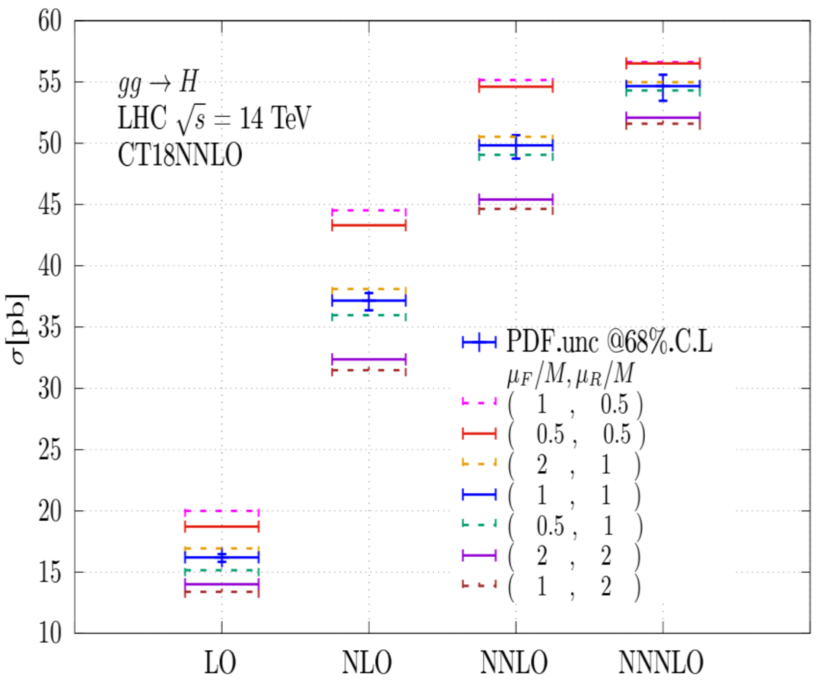

Tools : ggHiggs(Marco Bonvini)

$\sigma(gg \to H)$ at 14 TeV LHC

7-point scale variation at N3LO in QCD for $m_t = 172.5$ GeV and $M = m_H = 125$ GeV

μ_R/M \ μ_F/M	0.5	1	2
0.5	3.4%	3.6%	-
1	-0.6%	-	0.6%
2	-	-5.6%	-4.7%

- The K-factor of electroweak (EW) correction is about 1.05
- The PDF uncertainty is about 2.8%

Estimating missing higher order contribution via varying μ_f and μ_R scales

arXiv:2107.09085

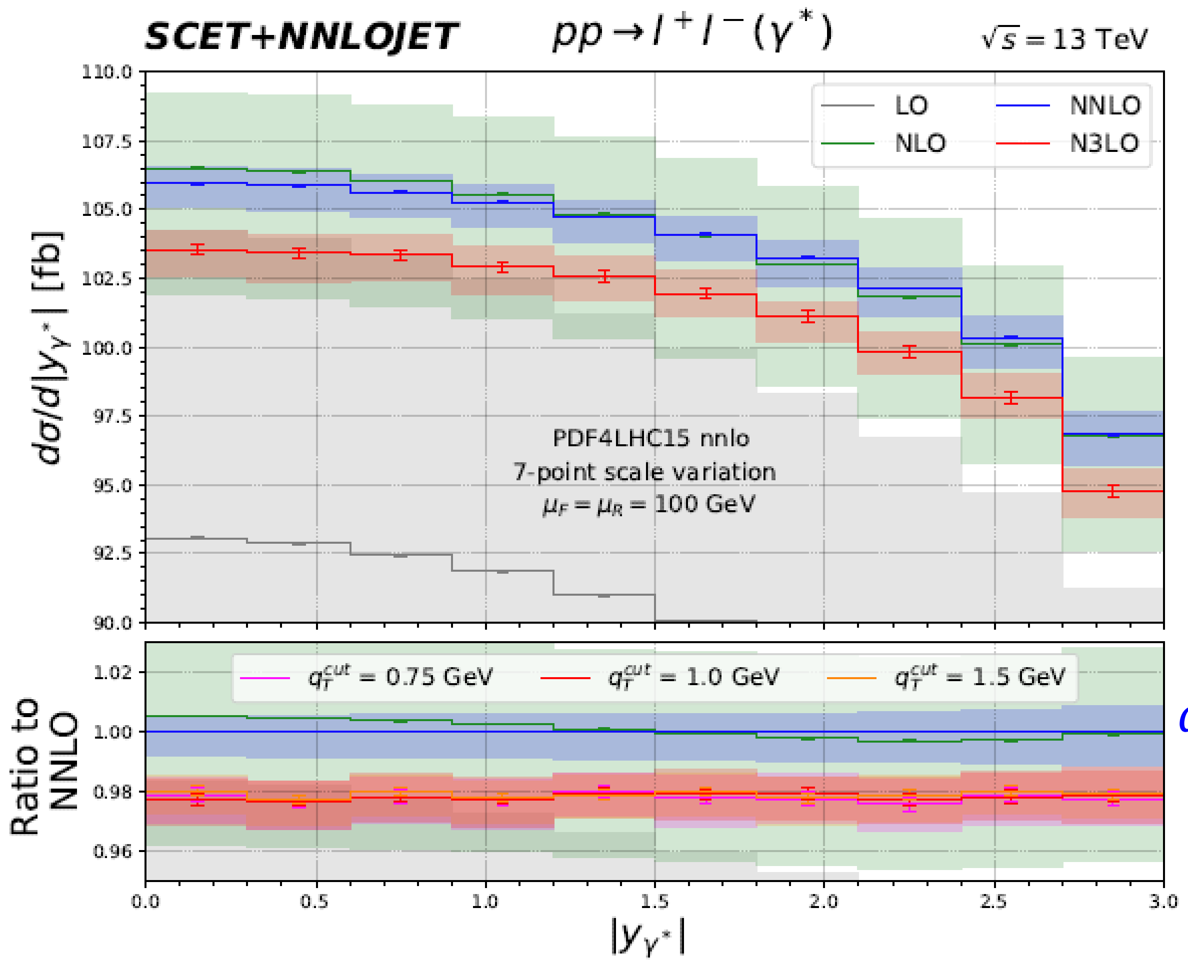

α_s^2

α_s^3

- Varying the factorization μ_f and renormalization μ_R scales by a factor of 2 around their nominal values (with 7-point scale variation) does not always lead to a good estimate of missing higher order (MHO) effect in the perturbative calculation.
- The N3LO correction is outside the scale variation band predicted at NNLO, due to accidental cancellation among various partonic subprocess contributions.

This comparison does not include PDF and α_s induced errors.

Some data requires all-order (resummation) calculations

- When applying a symmetric p_T cut (with same magnitude) on the decay leptons of inclusive W or Z boson production, the two leptons are almost back-to-back, decaying from a low p_T gauge boson.
- Fixed order predictions cannot correctly predict the low p_T distribution of W or Z.
- It requires a resummation calculation, such as ResBos, to resum all the large logs arising from multiple soft-gluon radiation.

What's QCD Resummation?

- Perturbative expansion

$$\frac{d\hat{\sigma}}{dq_T^2} \sim \alpha_s \left\{ 1 + \alpha_s + \alpha_s^2 + \cdots \right\}$$

- The singular pieces, as $\frac{1}{q_T^2}$ (1 or log's)

$$\frac{d\hat{\sigma}}{dq_T^2} \sim \frac{1}{q_T^2} \sum_{n=1}^{\infty} \sum_{m=0}^{2n-1} \alpha_s^{(n)} \ln^{(m)}\left(\frac{Q^2}{q_T^2}\right)$$

$$\sim \frac{1}{q_T^2} \{ \quad \alpha_s \left(\underline{L} + 1\right) \qquad L \equiv \ln\left(\frac{Q^2}{q_T^2}\right)$$

$$+ \alpha_s^2 \left(\underline{L^3} + \underline{L^2} + \underline{L} + 1\right)$$

$$+ \alpha_s^3 \left(\underline{L^5} + \underline{L^4} + \underline{L^3} + \underline{L^2} + \underline{L} + 1\right)$$

$$+ \cdots \quad \}$$

Resummation is to reorganize the results in terms of the large Log's.

ResBos + CT18 can describe well low $p_T(Z)$ region, with $p_T(Z) < 20$ GeV

$$\alpha_s \ln\left(\frac{Q^2}{q_T^2}\right) \sim 1$$

Compare to LHCb 13 TeV Z data; arXiv:2112.07458

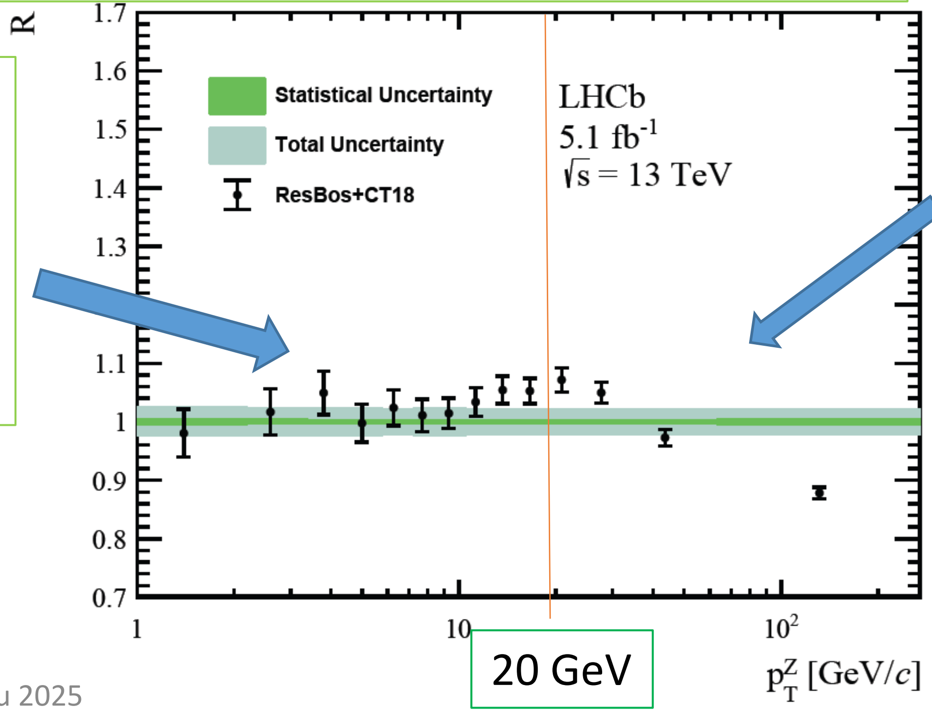

20 GeV

High $p_T(Z)$ region needs α_s^3 contrinution

Some data requires all-order (resummation) calculations: ResBos

Compare to ATLAS 8 TeV Z data; arXiv:1606.00689

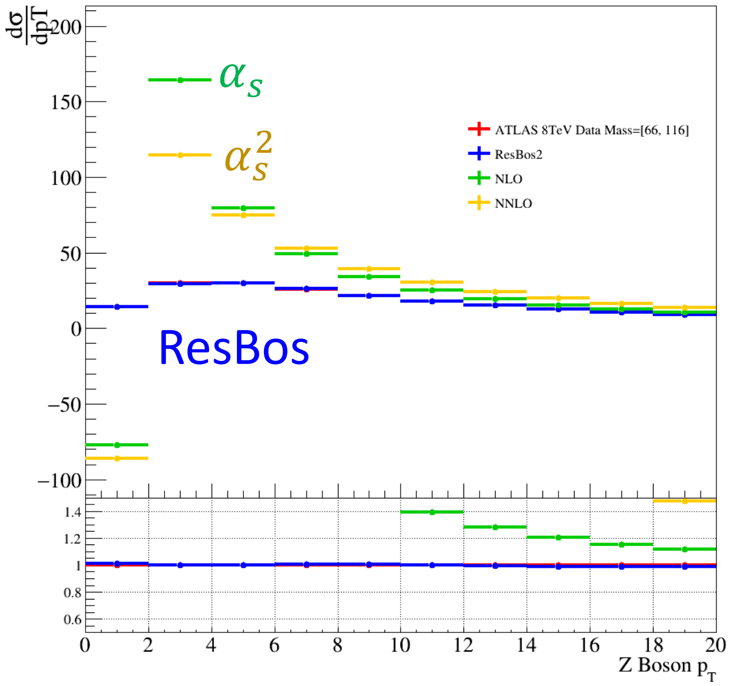

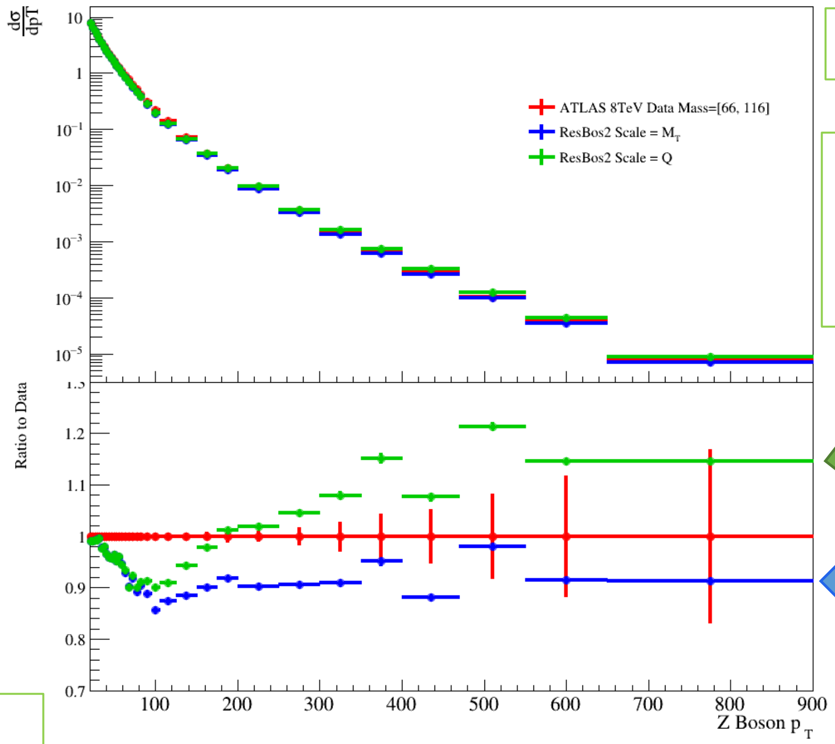

https://gitlab.com/resbos2

arXiv:2205.02788

- Sensitive to scale choices at α_s^2
- High $p_T(Z)$ region requires yet higher order (α_s^3) contribution.

Use $\mu_F = \mu_R = \mathrm{Q}$
Invariant mass, at α_s^2

Use $\mu_F = \mu_R = \mathrm{m_T}$
where $m_T = \sqrt{Q^2 + p_T^2}$
Transverse mass, at α_s^2

The low p_T Z data, with $p_T(Z) < 20$ GeV, can be described well by ResBos, but not fixed order (NLO, NNLO,…) calculations which yield singular result as $p_T(Z) \to 0$.

Require higher (fixed) order calculations for $p_T(Z) > 20$ GeV; α_s^3 correction increases the rate by about 10% when using the scale m_T and renders a good agreement with data.

Higher order contributions are important

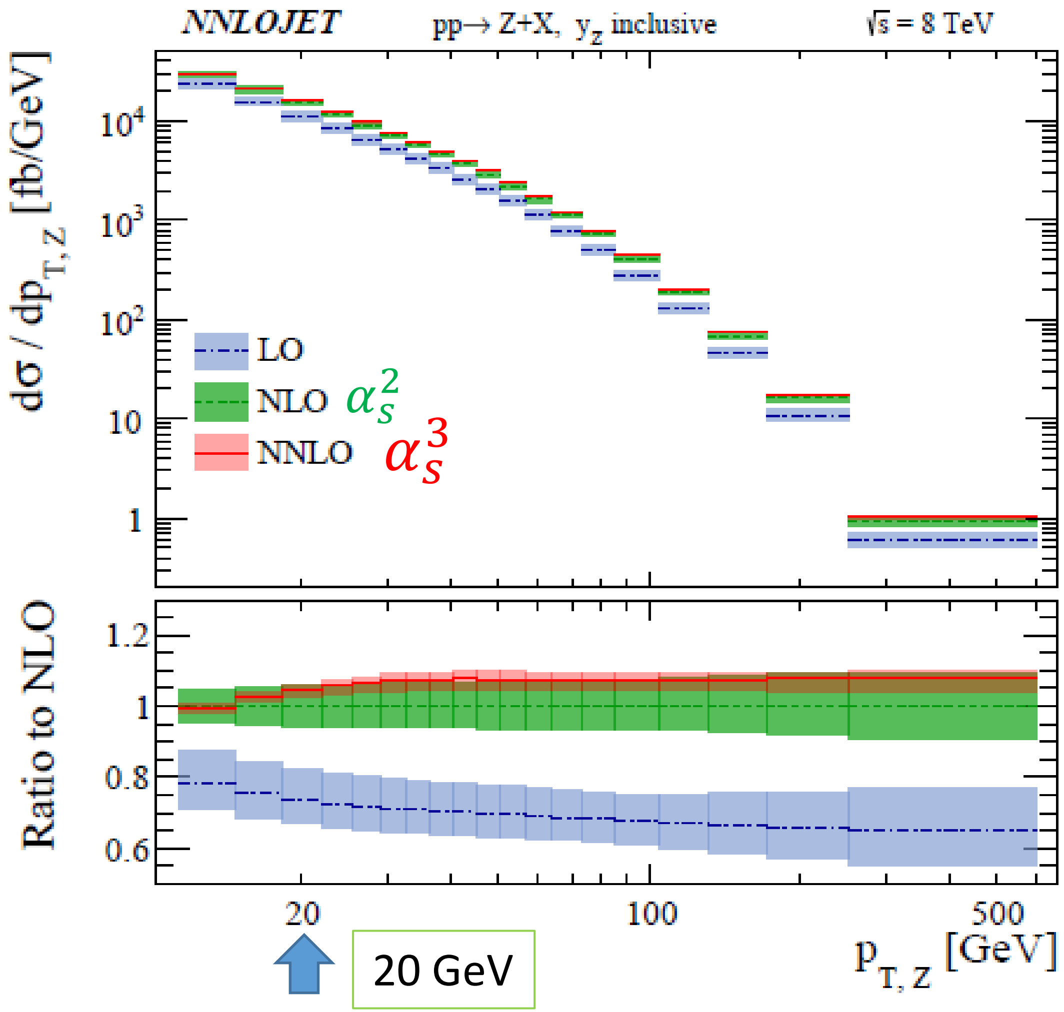

20 GeV

arXiv:1708.00008

- The α_s^3 prediction has much smaller scale variation as compared to α_s^2 calculation.
- For $p_{T(Z)} > 20$ GeV, the K-factor of α_s^3/α_s^2 is roughly a constant, about 1.1

Impact of SIDIS data

- Di-muon data
- Couple to final state fragmentation function and decay branching ratio

Scattering processes at the EIC

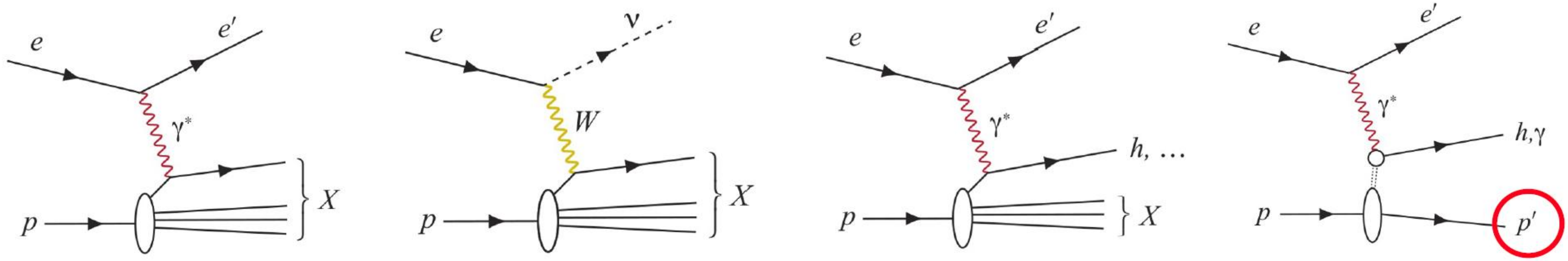

Neutral Current DIS **Charged Current DIS** **Semi-Inclusive DIS** **Exclusive Processes**

- Electron beam can be longitudinally polarized.
- Proton (Ion) beam can be longitudinally or transversely polarized.
- The measurements of exclusive processes are special at the EIC, as compared to the LHC.

Impact of NuTeV and CCFR SIDIS dimuon data

arXiv:1907.12177

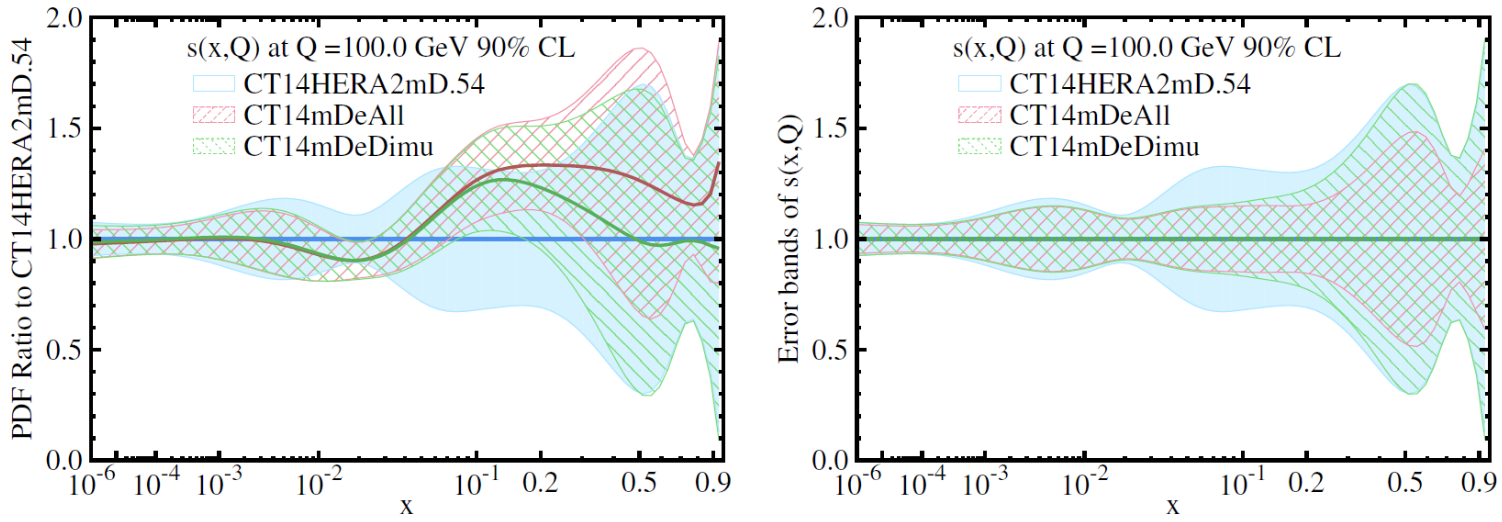

FIG. 16: Comparison of ePump-updated s-PDF, at $Q = 100$ GeV. CT14mDeDimu is obtained by adding only the DIS charged current dimuon data (NuTeV [18], and CCFR [19]) to CT14HERA2mD with ePump.

- NuTeV and CCFR di-muon data provide important constraints on s and $\bar{s}$ PDFs at large x.
- They are SIDIS data, so that constraints on PDFs depend on the modeling of final state fragmentation and the value of $c \to \mu$ decay branching ratio R.
- The LHC W and Z data can constrain s and $\bar{s}$ PDFs at $x \sim 10^{-2}$.

Impact of NuTeV and CCFR SIDIS dimuon data

arXiv:2211.11064

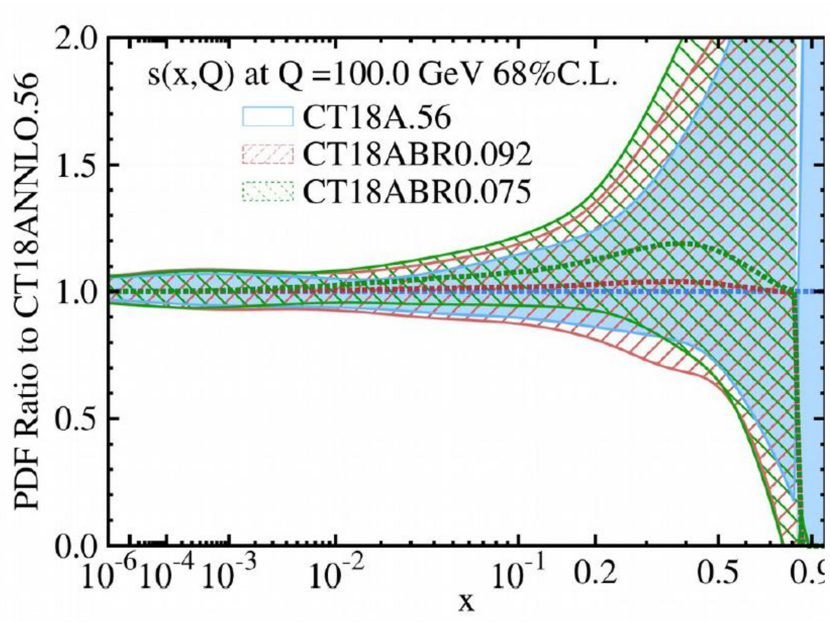

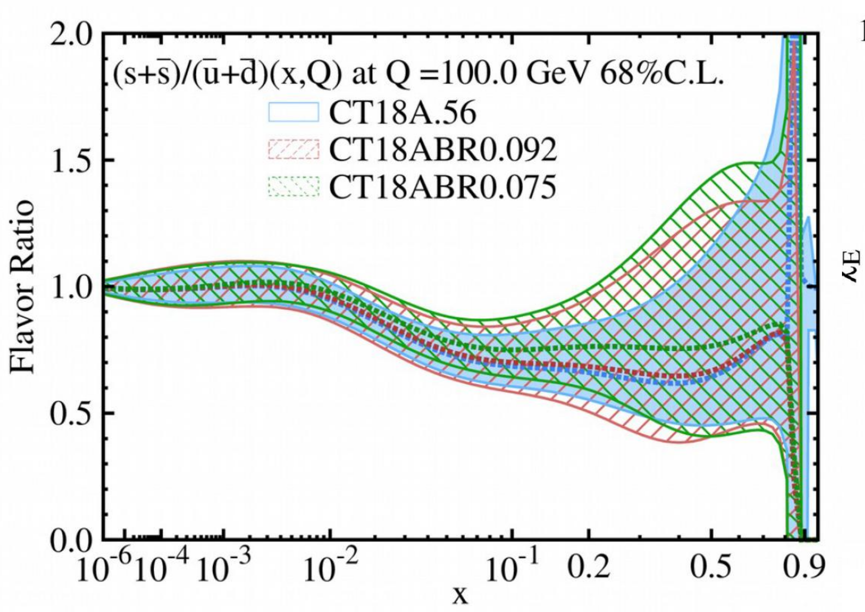

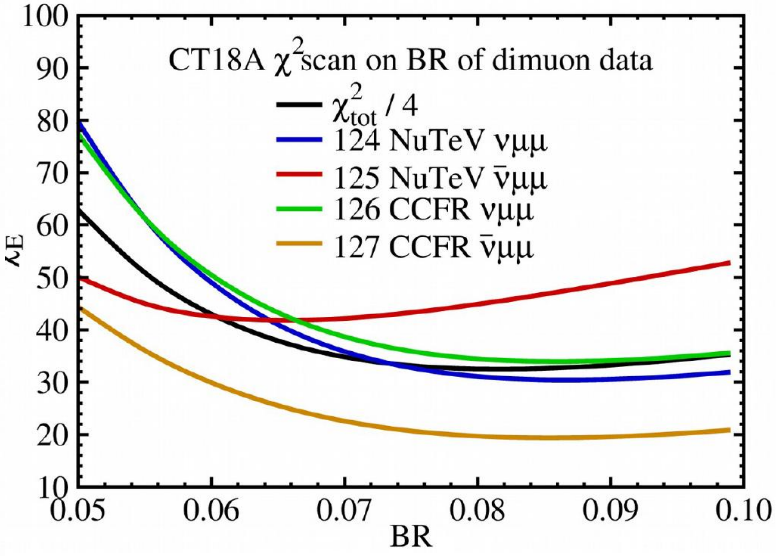

# fitname	248	124	125	126	127
CT18A	87.55	31.91	52.81	35.59	20.88
CT18ABR0.092	85.16	31.49	49.97	34.65	20.53
CT18ABR0.075	79.02	32.83	43.25	34.64	21.30

- In CT18A, the $c \to \mu$ decay branching ratio R is taken to be 0.099
- No noticeable changes by varying R from 0.099 to 0.092

(ID=248 refers to ATLAS 7 TeV W/Z data.)

Toward a new generation of CT2025 PDFs

- Identify sensitive, mutually consistent new experimental data sets using preliminary fits and fast techniques (L_2 sensitivities and $ePump$)
- Implement N3LO QCD and NLO EW contributions as they become available. N3LO accuracy is reached only when N3LO terms are **fully** implemented.
- Explore quark sea flavor dependence: $s-\bar{s}$ (CT18As), fitted charm (CT18FC),…
- Include lattice QCD constraints (CT18As_Lat)
- Next-generation PDF uncertainty quantification: META PDFs, Bézier curves, MC sampling, multi-Gaussian combination, …
- Lattice QCD: Provides constraints on hadron structures not currently accessible experimentally, e.g., $s-\bar{s}$ and g PDFs at large x.

Backup slides

ePIC performance: DIS kinematics with ePIC

Kinematic Resolutions

$$y_e = 1 - \frac{E_e(1-\cos\theta_e)}{2E_0}, \qquad Q_e^2 = 2E_0E_e(1+\cos\theta_e).$$

$$y_{DA} = \frac{\alpha_h}{\alpha_e+\alpha_h}, \qquad Q_{DA}^2 = \frac{4E_0^2}{\alpha_e(\alpha_e+\alpha_h)}$$

$$y_\Sigma = \frac{\delta_h}{\delta_h + E_e(1-\cos\theta_e)}, \qquad Q_\Sigma^2 = \frac{E_e'^2\sin^2\theta_e}{1-y_\Sigma}.$$

- Reconstruct inclusive kinematics using various methods
  → **compare reconstruction performance**
  - Color of point indicates best method for *y* (inelasticity)
  - Size of point indicates *y* resolution
- **~30% or better *y* resolution across $x - Q^2$ plane**

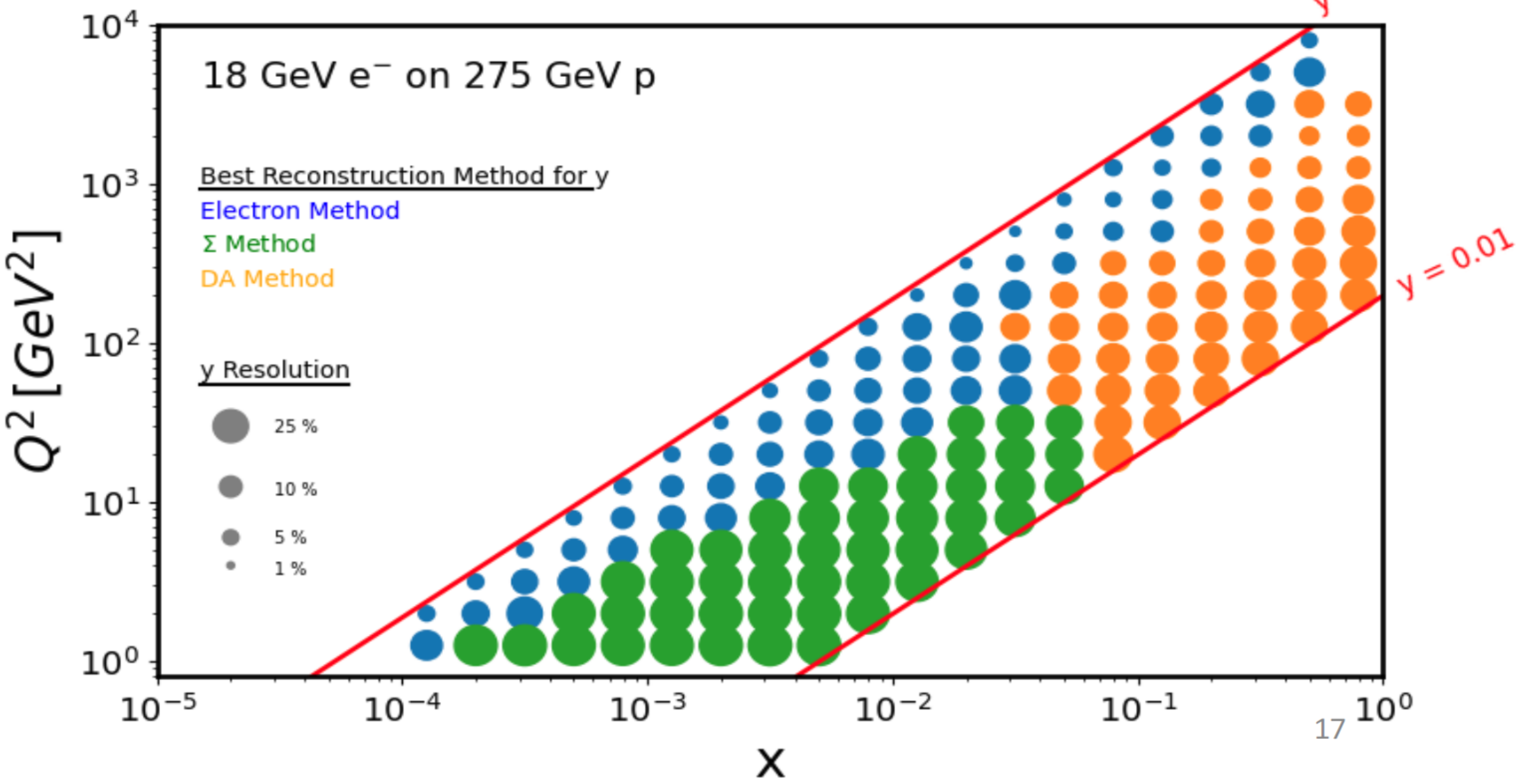

S Fazio, BNL-INT Joint Workshop, June 2025

Leading Twist TMDs

Nucleon Spin   Quark Spin

arXiv: 1212.1701

C T E Q

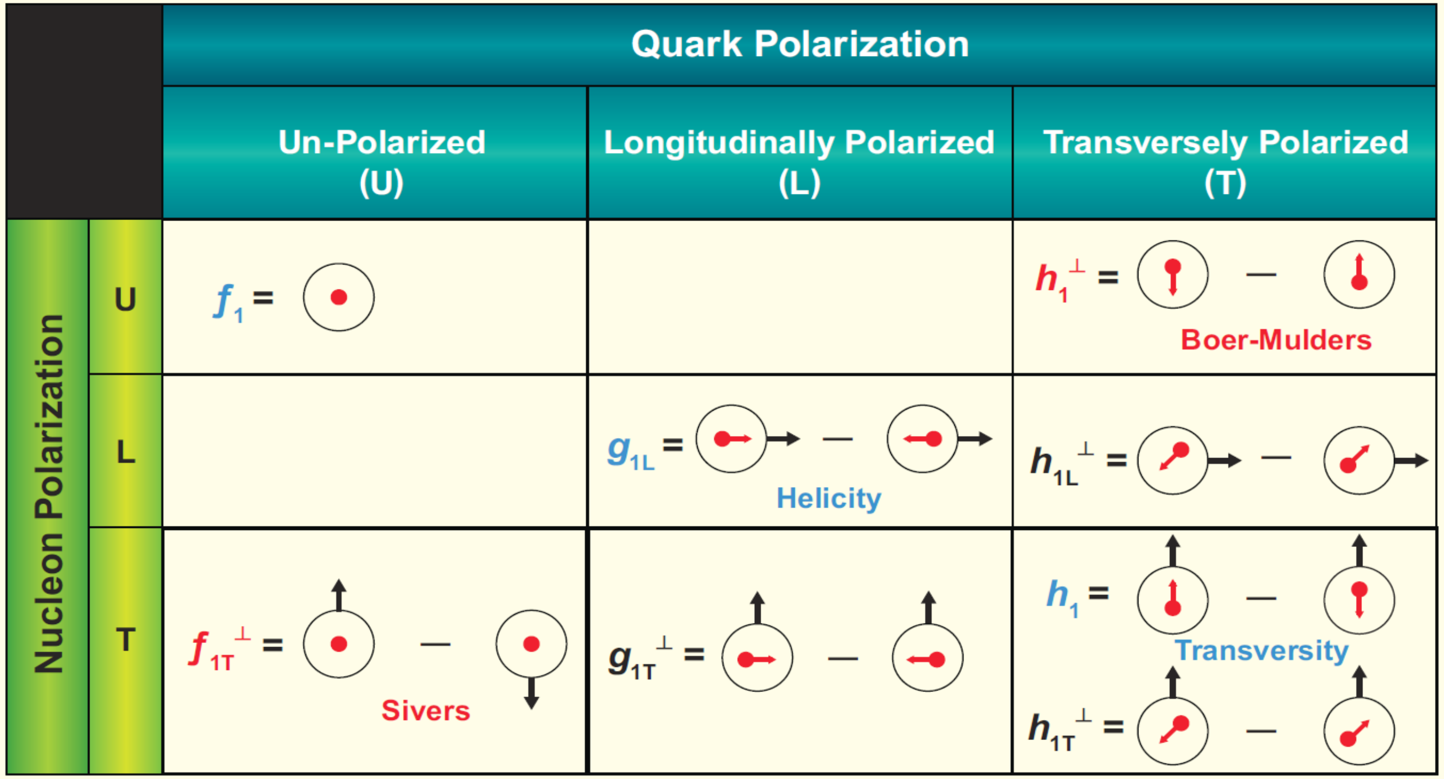

Figure 2.12: Leading twist TMDs classified according to the polarizations of the quark (f, g, h) and nucleon (U, L, T). The distributions $f_{1T}^{\perp,q}$ and $h_1^{\perp,q}$ are called naive-time-reversal-odd TMDs. For gluons a similar classification of TMDs exists.

The differential SIDIS cross section can be written as a convolution of the transverse momentum dependent quark distributions $f(x, k_T)$, fragmentation functions $D(z, p_T)$, and a factor for a quark or antiquark to scatter off the photon. At the leading power of $1/Q$, we can probe eight different TMD quark distributions as listed in Fig. 2.12. These distributions represent various correlations between the transverse momentum of the quark $\boldsymbol{k}_T$, the nucleon momentum $\boldsymbol{P}$, the nucleon spin $\boldsymbol{S}$, and the quark spin $\boldsymbol{s}_q$.